



Title	Relaxation Effects in Antiferromagnetic Resonance
Author(s)	Yamazaki, Hitoshi
Citation	大阪大学, 1967, 博士論文
Version Type	VoR
URL	https://hdl.handle.net/11094/2379
rights	
Note	

The University of Osaka Institutional Knowledge Archive : OUKA

<https://ir.library.osaka-u.ac.jp/>

The University of Osaka

Relaxation Effects in Antiferromagnetic Resonance

Hitoshi YAMAZAKI

Feb. 20, 1967

Contents

Abstract.	2
1. Introduction.	3
2. Crystal structure and spin orientation.	7
3. Experimental method.	8
4. Results and discussions.	17
a) Shift in the resonance position.	18
b) Linewidth.	29
c) Measurements of M_z and the relaxation times.	34
d) Measurements of χ'' and $M_{x,y}$	50
e) Energy transfer model.	53
5. New antiferromagnetic resonance lines in $\text{CuCl}_2 \cdot 2\text{H}_2\text{O}$	55
References.	59

Abstract

Various relaxation times observed in antiferromagnetic resonance of $\text{CuCl}_2 \cdot 2\text{H}_2\text{O}$ were investigated experimentally. Both pulsed and continuous high power microwaves of about 160 milli-watts were applied to the single crystal at low temperatures and the rise and decay times of the induced magnetization M_z , shift of the resonance line, and complex susceptibilities χ' and χ'' were investigated in detail. Three characteristic relaxation times were specified. The transverse component $M_{x,y}$ decays with relaxation time T_2 of about 10^{-8} sec while the longitudinal component M_z relaxes with T_{1a} of about 10^{-7} sec. An empirical formula for T_{1a} was obtained as $T_{1a} = (1.1 \pm 0.1) \times 10^{-6} T^{-(5.0 \pm 0.5)}$ which is considered as the spin-lattice relaxation time. Another relaxation time T_{1b} of the order of $10^{-3} \sim 10^{-5}$ sec was also observed and the origin of this relaxation is attributed to the lattice-bath heat transfer relaxation.

1. Introduction.

Relaxation mechanism in antiferromagnetic crystals is yet almost unknown, while that in para- and ferro-magnetic materials has been investigated considerably. One of the reasons for this is that antiferromagnets suitable for a precise analysis of the relaxation mechanism, as YIG with regard to ferromagnetic relaxation, are hard to find. Since the linewidth in antiferromagnetic resonance is a measure by which one should be able to infer the relaxation mechanism, measurements of it have been done in several materials^{1)~3)} with varying temperature. The corresponding theory is, however, not complete, theories hitherto published being in disagreement with one another. The linewidth resulting from the interaction of the uniform precession of the magnetization with spin-wave has been studied theoretically, on the basis of four-magnon precesses, by Genkin and Fain,⁴⁾ by Kawasaki,⁵⁾ by Harris,⁶⁾ and by several others.^{7)~9)} Loudon and Pincus¹⁰⁾ treated the effect of dipolar interaction and estimated, on the basis of two-magnon processes, the linewidth arising from some types of point imperfections and pits. A theoretical study of two-magnon one-phonon processes for the temperature dependence of the spin-lattice relaxation time was performed by Upadhyaya and Sinha.¹¹⁾ On the other hand, attempts have been done to investigate the relaxation by observing a nonlinear effect appearing in the antiferromagnetic resonance in $\text{CuCl}_2\cdot 2\text{H}_2\text{O}$,¹²⁾ KMnF_3 ,¹³⁾ and MnCO_3 .¹⁴⁾ Heeger¹³⁾ has pointed out that the nonlinear effect may be due to the onset of spin-

wave instability analogous to that of a ferromagnet, and he estimated the spin-wave linewidth of KMnF_3 . Various types of nonlinear dynamic phenomena in antiferromagnets were theoretically studied by Ozhigin.¹⁵⁾ Recently Naiman et al.¹⁶⁾ measured the spin-flop relaxation time near the critical field H_c in $\text{CuCl}_2\cdot 2\text{H}_2\text{O}$.

In order to investigate the relaxation mechanism in an antiferromagnetic spin system, we tried to observe directly the behaviour of the longitudinal and transverse magnetic moments, M_z and $M_{x,y}$. We observed the magnetic flux change induced by the resonance when a pulsed microwave was applied to an antiferromagnet, $\text{CuCl}_2\cdot 2\text{H}_2\text{O}$. This is similar to the observation made by Damon¹⁷⁾ and Bloembergen and Wang¹⁸⁾ for the study of the ferromagnetic relaxation in some ferrites. The specimens used are single crystals of $\text{CuCl}_2\cdot 2\text{H}_2\text{O}$. The reason why we adopted this compound is that the minimum value of the antiferromagnetic resonance full-linewidth was about 7 Oe, which is the narrowest of all observed so far in antiferromagnetic resonance. Accordingly, this compound may be considered as one of the best substances for studying the relaxation. Antiferromagnetic properties of this compound have been well investigated: the magnetic susceptibility was measured by Van der Marel et al.,¹⁹⁾ the specific heat by Friedberg,²⁰⁾ the proton magnetic resonance by Poulis et al.,²¹⁾ and the neutron diffraction by Shirane et al.²²⁾²³⁾ Detailed measurements of antiferromagnetic resonance in $\text{CuCl}_2\cdot 2\text{H}_2\text{O}$ were made by the Leiden group²⁴⁾ more than ten years ago. Afterwards, more precise measurements were performed by Date and Nagata.²⁵⁾ Their results were well understood by

the theory developed by Nagamiya and Yosida,²⁶⁾ by Ubbink,²⁷⁾ and by Date and Nagata.²⁵⁾ Recently, new resonance lines were found near the a-axis by the present author,²⁸⁾ though the origin of the lines was not yet clear. It is known that $\text{CuCl}_2 \cdot 2\text{H}_2\text{O}$ has an orthorhombic anisotropy energy which arises from dipolar and anisotropic exchange interactions,²⁹⁾ does not have one-ion type anisotropy energy because of $S = \frac{1}{2}$, and possibly has a canted antiferromagnetic spin arrangement due to an antisymmetric anisotropic spin coupling.³⁰⁾

Now let us consider an induced magnetization due to resonance. As is well known, the total magnetization is zero at 0°K when an external magnetic field H is applied along the spin easy axis z , if $H < H_c$. In the state of resonance, however, the magnetizations M_x , M_y , and M_z are not zero. In this case there are two resonance modes, i.e., the low- and high-frequency modes (see Eq.(2)). The steady state orientations of the sublattice magnetizations in the low-frequency mode, whose relaxation effects were investigated in this paper, are shown in Fig.1. When a microwave, whose frequency satisfies the resonance condition, is applied stepwise from the time $t=0$, the transverse components M_x and M_y begin to oscillate with the microwave frequency, while M_z rises from zero up to an equilibrium value, with a relaxation time T_1 , according to

$$M_z(t) = M_z^0 \left\{ 1 - \exp(-t/T_1) \right\} \quad (1)$$

where M_z^0 means the equilibrium magnetization along the z -axis induced by the resonance. A similar relaxation effect is also seen when the microwave is cut off. In this paper various

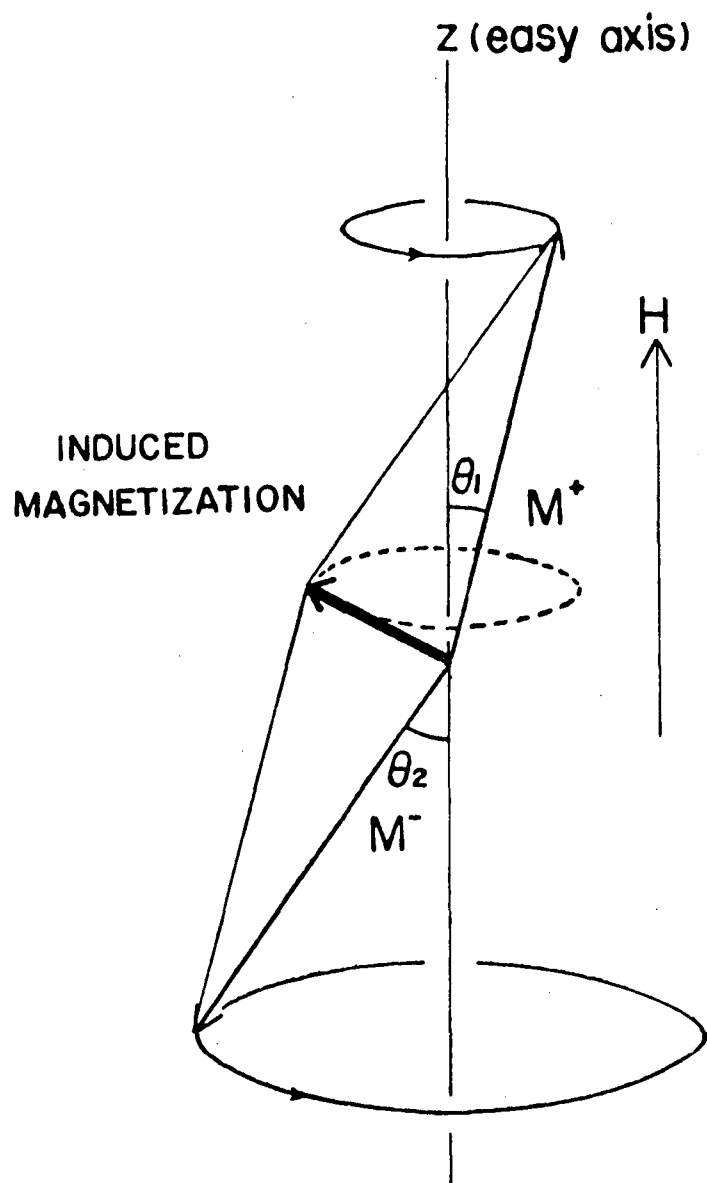


Fig.1 Equilibrium orientations of the magnetization of the low-frequency mode ω_l .

characteristics of M_z and its relaxation time will be discussed, together with the resonance shift, line broadening, phenomenological χ' and χ'' near the resonance.

2. Crystal structure and spin orientation.

The crystal structure of $\text{CuCl}_2 \cdot 2\text{H}_2\text{O}$ is well known; it is orthorhombic with lattice parameters $a = 7.38\text{\AA}$, $b = 8.04\text{\AA}$, and $c = 3.72\text{\AA}$. There are two copper ions in the chemical unit cell at $(0,0,0)$ and $(\frac{1}{2}, \frac{1}{2}, \frac{1}{2})$. Below the Néel temperature of 4.31°K , the spins of the Cu^{++} ions take an antiferromagnetic arrangement, which was studied by a proton resonance experiment by Poulis and Hardeman.²¹⁾ Within the limit of the analysis of the experiment, it was known that all the spins in each ab-plane are parallel to each other and they are antiparallel to the spins in the ab planes immediately above and below. This spin superstructure was confirmed by a neutron diffraction experiment by Shirane et al.²²⁾ The direction of easy magnetization is the a-axis. In the unit cell there are four water molecules at $(0, \pm u, 0)$ and $(\frac{1}{2}, \frac{1}{2} \pm u, 0)$, with $u=0.25$, and four chlorine ions at $(\pm u, 0, \pm v)$ and $(\frac{1}{2} \pm u, \frac{1}{2}, \pm v)$, with $v=0.37$. The copper ions are subjected to an approximately orthorhombic crystalline field which has different orientations for the corner and base-centered ions. One of the principal axes of the field coincides with the b-axis of the crystal while the other two axes are rotated about the b-axis, away from the a- and c-axes, by an angle of -38° for the corner

ions and $+38^\circ$ for the base-center ions. Thus the two magnetic ions in a chemical cell are crystallographically inequivalent. Moriya³⁰⁾ proposed the canted spin arrangement for this crystal from his theory of antisymmetric spin coupling. Recently Umebayashi et al.²³⁾ performed a neutron diffraction experiment on $\text{CuCl}_2\cdot 2\text{D}_2\text{O}$ and obtained a canted component of about $0.1\mu_B$. The crystal structure and spin arrangement are shown in Fig.2. The angle of spin canting may be of the order of several degrees in $\text{CuCl}_2\cdot 2\text{H}_2\text{O}$ and is not shown in the figure.

3. Experimental method.

The specimens used in this experiment were grown at room temperature gradually from the saturated aqueous solution of pure copper chloride. The process took more than one month. Green single crystals having well-developed (110) faces were obtained, which have a needle-like shape and show a perfect cleavage along the c-plane. To prevent deliquescence, the single crystals were preserved in pure clock oil. The weight of the single crystals usually used in the experiment was 2~4 mg. A sample of 50 mg was used in order to determine a long M_z relaxation time of millisecond order.

Fig.3 is the block diagram of the experimental system. A pulsed microwave of X band with rise and decay times of about 3×10^{-8} sec was applied to TE_{101} rectangular cavity. The microwave power was supplied by a V-58 klystron which was modulated by a pulsed voltage applied to the repeller electrode, and the

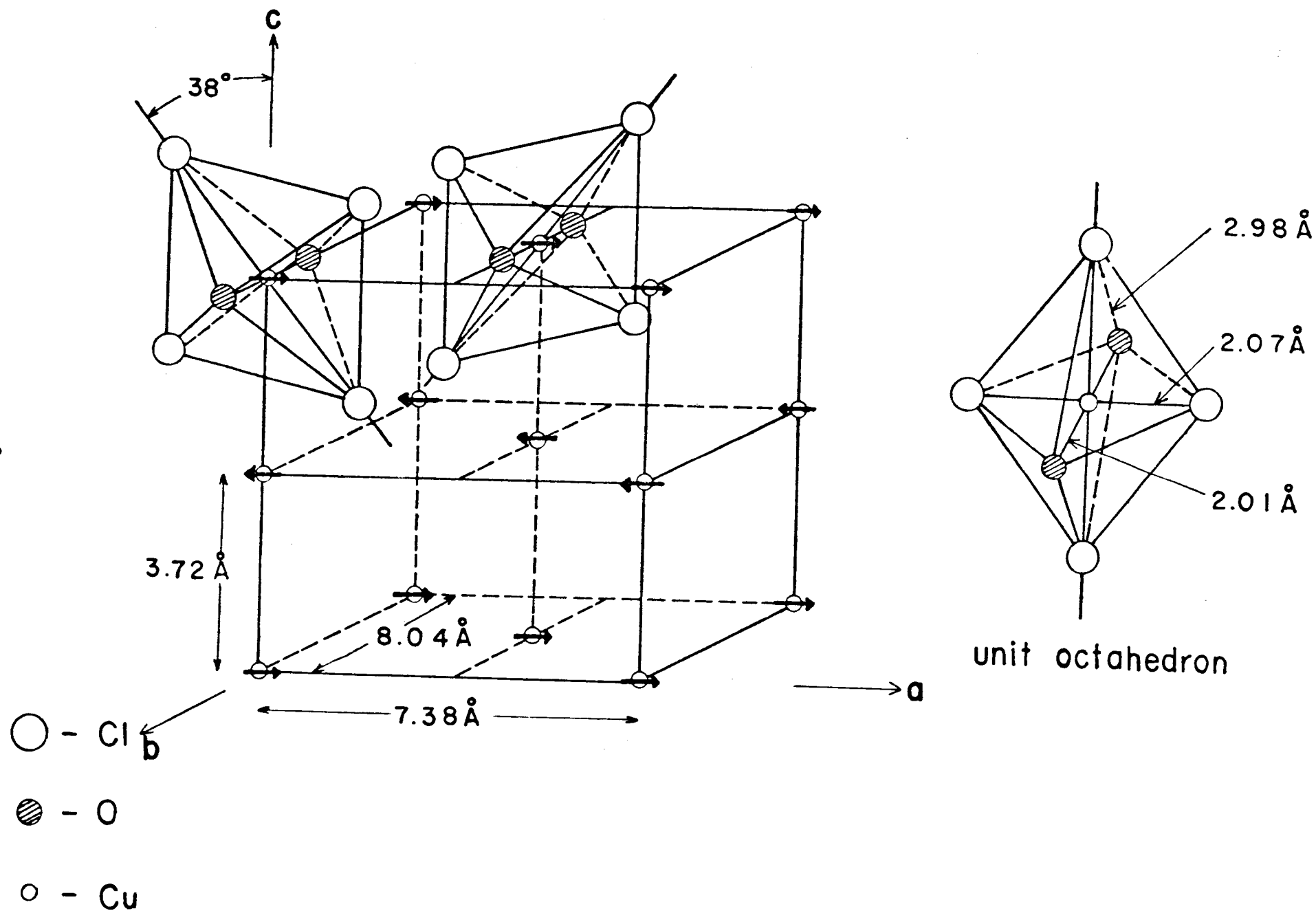
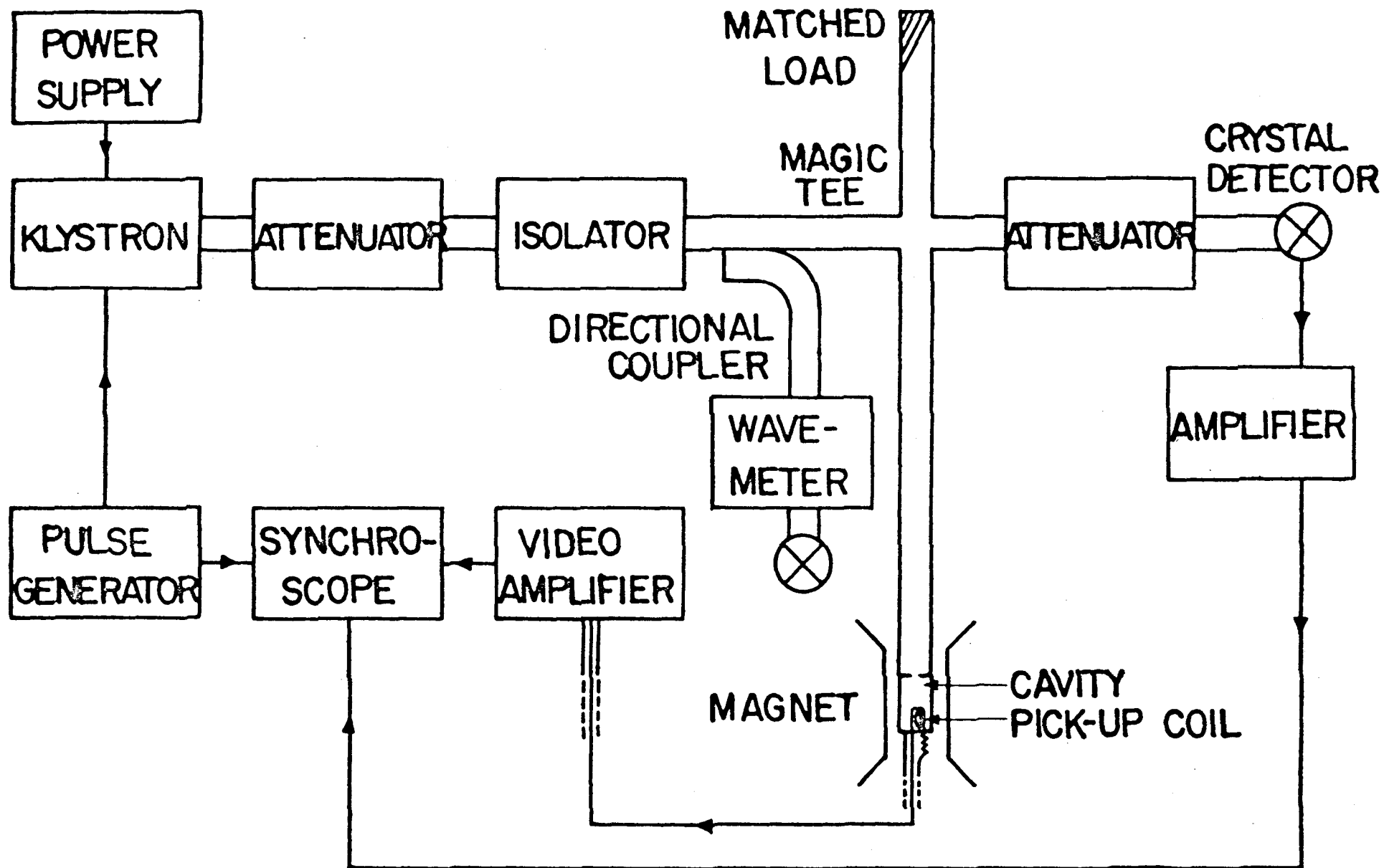


Fig.2 Crystal and spin structure of antiferromagnetic $\text{CuCl}_2 \cdot 2\text{H}_2\text{O}$

Fig. 5 Block diagram of equipment.



maximum power feeded in the cavity was about 160 mW. An impedance matched pick-up coil of 10 turns and 3.5 mm in diameter was placed inside the cavity so as to catch the flux change induced by the resonance. The coil is connected by a coaxial line to a video amplifier, the output of which can be displayed on a synchroscope. In order to observe a short relaxation time of $\sim 10^{-8}$ sec, it is important that the impedance of a pick-up coil is equal to that of a coaxial cable. The wave shape of the signal at various points in the detecting system is shown in Fig.4. The gain characteristics of the video amplifier is flat at 60 db up to about 30 Mc/sec. Typical signals are shown in Fig.5. The voltage induced in the pick-up coil is proportional to dM_z/dt . The Q of ^{the} cavity wherein a pick-up coil was placed, was 1200, while the Q without a pick-up coil was 1400, ^{both} at liquid helium temperature. If a pick-up coil was placed outside the cavity, it ^{would be} difficult to catch a small M_z signal. But as we cannot place a large coil inside the cavity for measuring M_z which ^{has} a long relaxation time, another pick-up coil of 0.5 mH was placed near the slit outside the TE₁₀₁ cavity. Fig.6 ^{(a) and (b)} shows the relative positions of the cavity, the sample, and the pick-up coils. The transverse component of the magnetization $M_{x,y}$ was detected by a one turn pick-up coil placed on the bottom of the cavity as is shown in Fig.6(c). The pick-up coil catch the microwave voltage induced by the resonance and the voltage is introduced to a coaxial cable-wave guide convertor and hence to a crystal detector.

When a continuous microwave of 160 mW was feeded in the cavity, the helium bath temperature was raised by 0.25°K from 1.48°K.

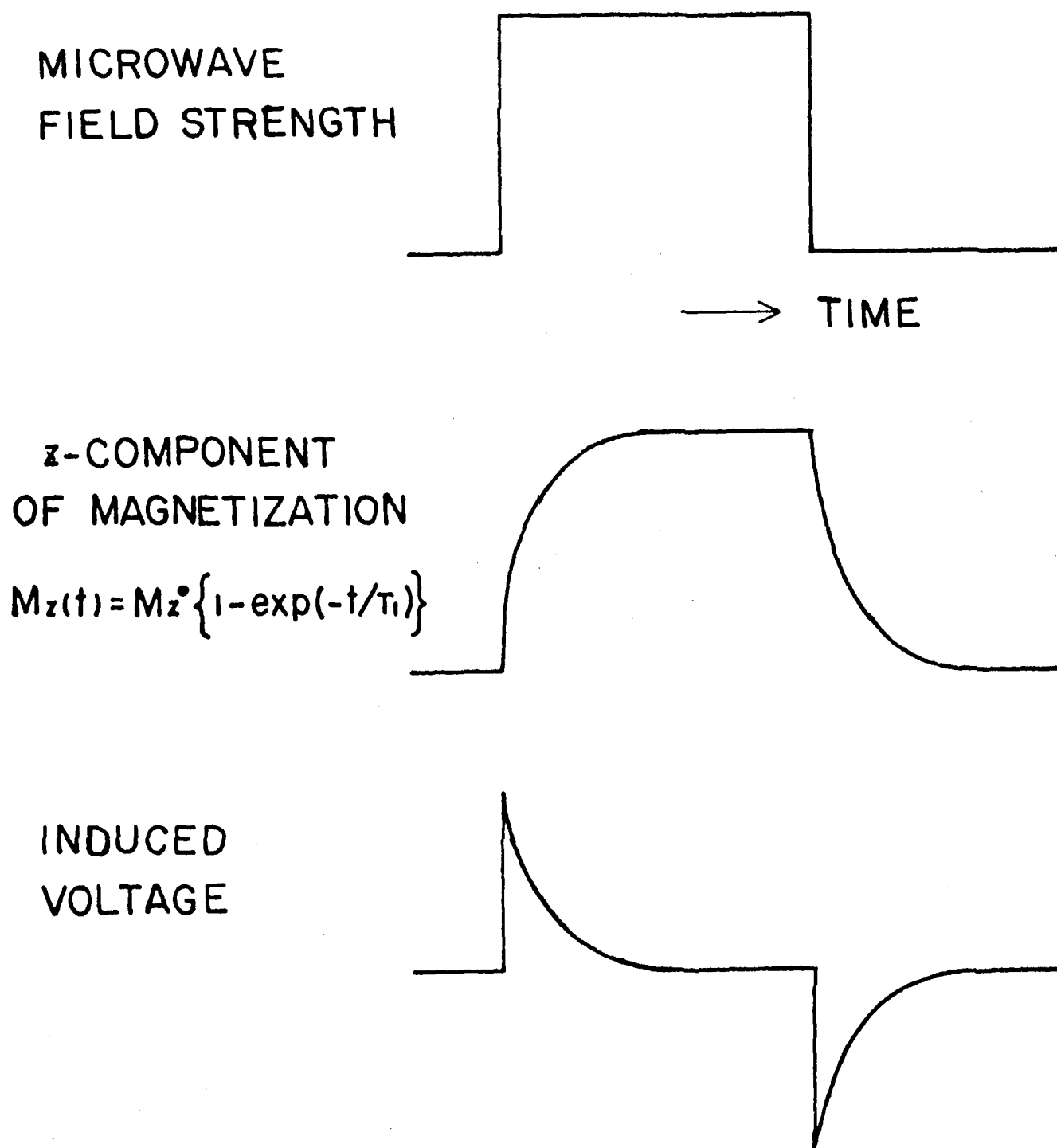
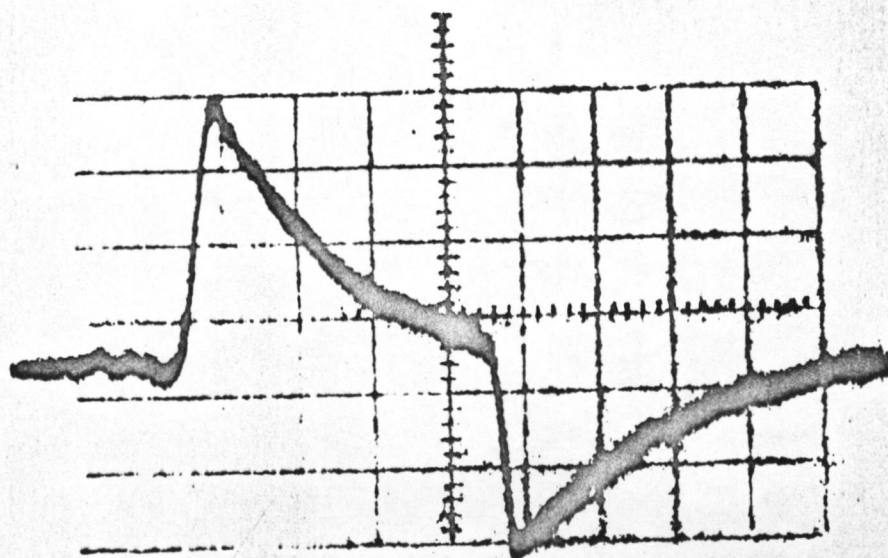
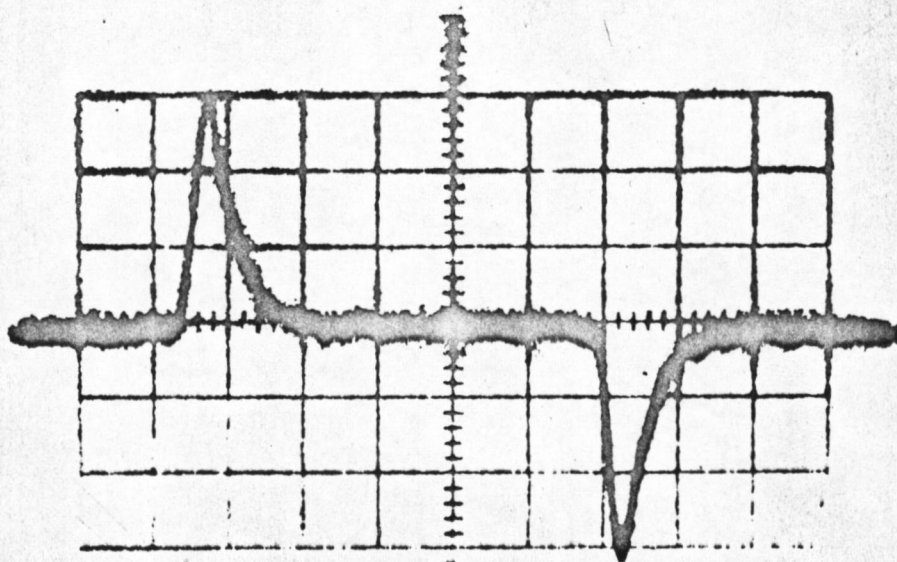


Fig.4 M_z signal at some points in detecting system.



(a)



(b)

Fig.5 The induced signal by the change of M_z .

(a) $T=1.4^\circ\text{K}$, (b) $T=1.9^\circ\text{K}$ (10^{-7} sec per division)

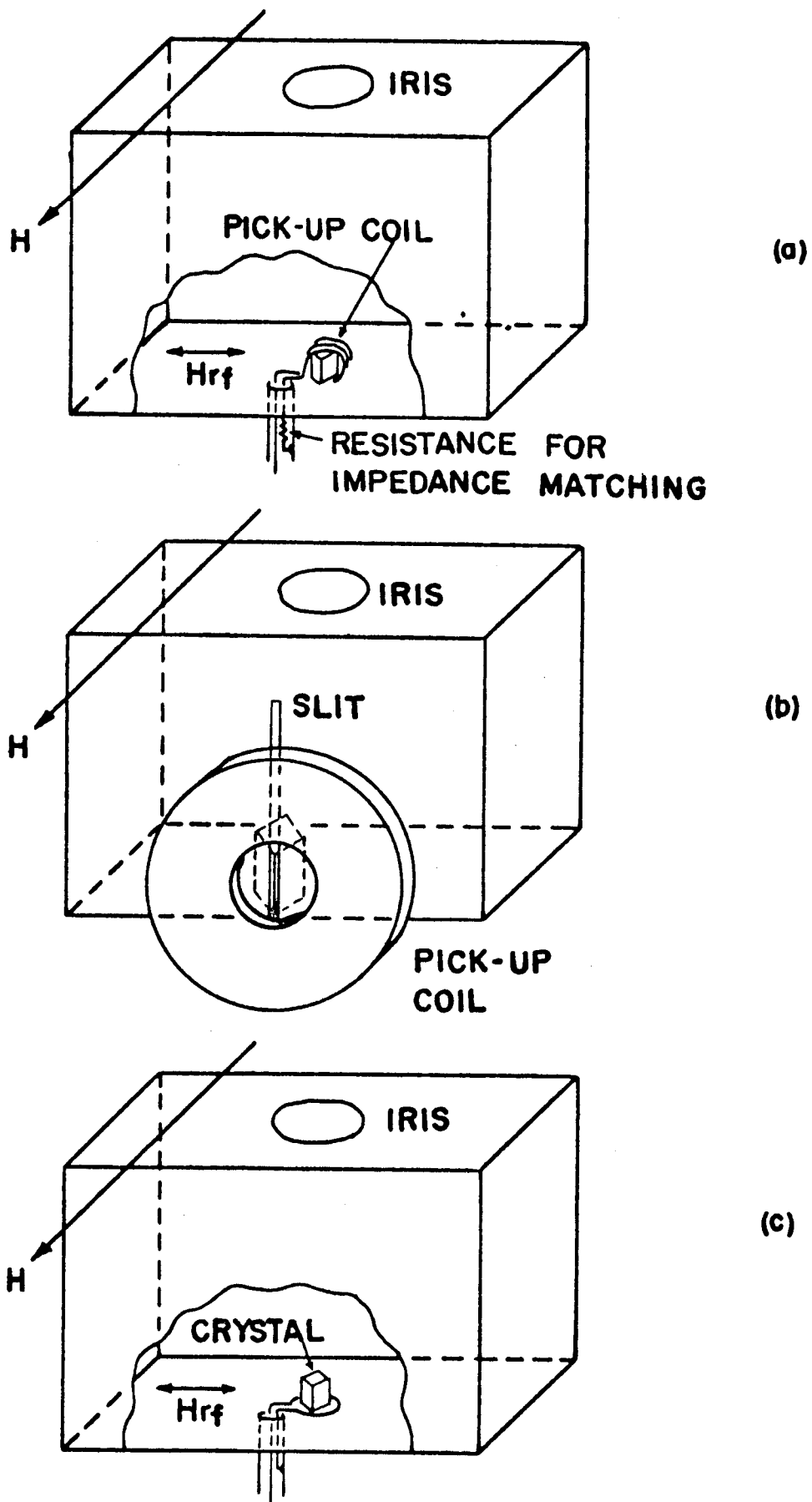


Fig.6 Relative positions of cavity, sample, and pick-up coil for measuring M_z and T_1 (a, b) and $M_{x,y}$ (c).

This heating comes from the joule loss in the microwave skin depth of the wave guide and cavity. The bath temperature was measured by a carbon thermometer which was carefully shielded from microwave and placed near the cavity. The carbon thermometer of 50 ohm at room temperature was calibrated against the vapour pressure of liquid helium. By using the critical field H_c for the spin flopping as an indicator of the spin temperature, it is found that the spin temperature at off resonant condition accords with the bath temperature measured by the carbon thermometer. H_c was determined as follows: a pick-up coil for measurements of M_z was connected to a Pound-Knight type NMR detector because the NMR detector can sensitively detect the change in the magnetization accompanying the spin flop transition. When a microwave is applied stepwise ^{from} the time $t=0$, the bath temperature and also the spin temperature rise gradually to an equilibrium temperature. A similar effect is also seen when the microwave is cut off. An observed time dependence of the bath and the spin temperature is shown in Fig.7. The characteristic time is about 60 sec. Of course this heating effect can be rejected when pulsed microwaves are used.

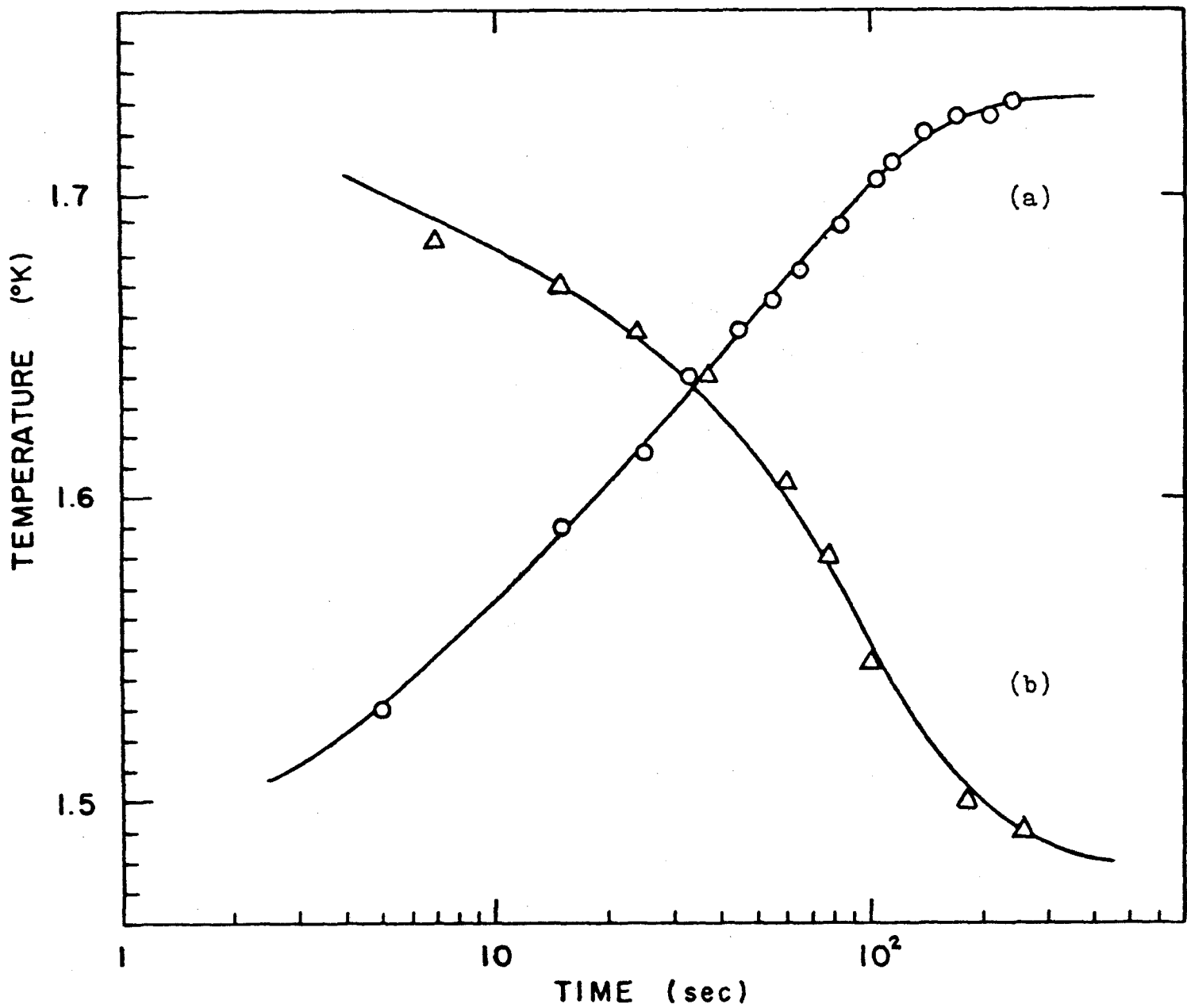


Fig. 7 Time dependences of bath temperature when a microwave is applied stepwise (a) and is cut off (b).

4. Results and discussions.

When the external field H is applied along the spin easy axis z and is smaller than H_c , the resonance frequency ω of antiferromagnetic resonance in $\text{CuCl}_2 \cdot 2\text{H}_2\text{O}$ is given by²⁶⁾

$$\left(\frac{\omega}{\gamma}\right)^2 = \frac{1}{2} \left[(1+\alpha^2)H^2 + C_1 + C_2 \pm \left\{ (1-\alpha^2)^2 H^4 + 2(1+\alpha)^2 H^2 (C_1 + C_2) + (C_1 - C_2)^2 \right\}^{1/2} \right], \quad (2)$$

where γ is the gyromagnetic ratio and α is the coefficient defined by

$$\alpha = 1 - \chi_{\parallel}/\chi_{\perp}, \quad (3)$$

where χ_{\parallel} is the susceptibility when H_0 is applied parallel to z and χ_{\perp} is the susceptibility when H_0 is applied perpendicular to z . Furthermore,

$$C_1 = 2AK_1, \quad C_2 = 2AK_2, \quad (4)$$

where A is the exchange constant of the molecular field approximation and K_1 and K_2 are the anisotropy energy constants along the b - and c -axes, respectively. The upper and lower signs before the $\{ \}$ in Eq.(2) correspond to the high-frequency mode ω_h and the low-frequency mode ω_l , respectively. We studied the relaxation effect of the low-frequency mode with a frequency at 9.0 kMc/sec, and the corresponding resonance field is 5.0 kOe at 1.4°K. At this frequency, another resonance can be observed when H is 7.1 kOe ($H > H_c$). But this mode is inadequate to study the relaxation because the linewidth is anomalously large and this line is closely related to the new resonance lines.²⁸⁾ found near the a -axis. The resonance

diagram and linewidth of the new lines will be appeared in the section 5. The frequency-field diagram when an external magnetic field is applied along the principal axes are shown in Fig.8. Van Till et al.¹²⁾ first observed a shift in antiferromagnetic resonance field of $\text{CuCl}_2 \cdot 2\text{H}_2\text{O}$ at high microwave power but they did not precisely analyzed the high power effect of the resonance.

We started ^{with} an experiment for high power effect of the antiferromagnetic resonance, using continuous microwave. As the results of the experiments, we found that both χ'' and χ' declined with increasing microwave magnetic field h_1 , that is to say, ^asaturation effect occurred ^r and that the resonance position shifted toward higher field with increasing h_1 and it terminated in a discrete jump of the resonance line to some other position as had been found by Van Till et al. In the case of high power experiment using continuous wave, the heating effect of both the lattice and the spin system should be considered carefully. As will be mentioned ⁱⁿ section 3, helium bath temperature is raised by a continuous microwave but this heating effect can be rejected by using pulsed microwaves. ^{Thus,} afterwards, the experiment was performed by using pulsed microwaves whose duty ratio was decreased until it was able to ignore the heating effect.

a) Shift in the resonance position.

It is frequently observed that the antiferromagnetic resonance point observed at the end of the microwave pulse (MP_f)

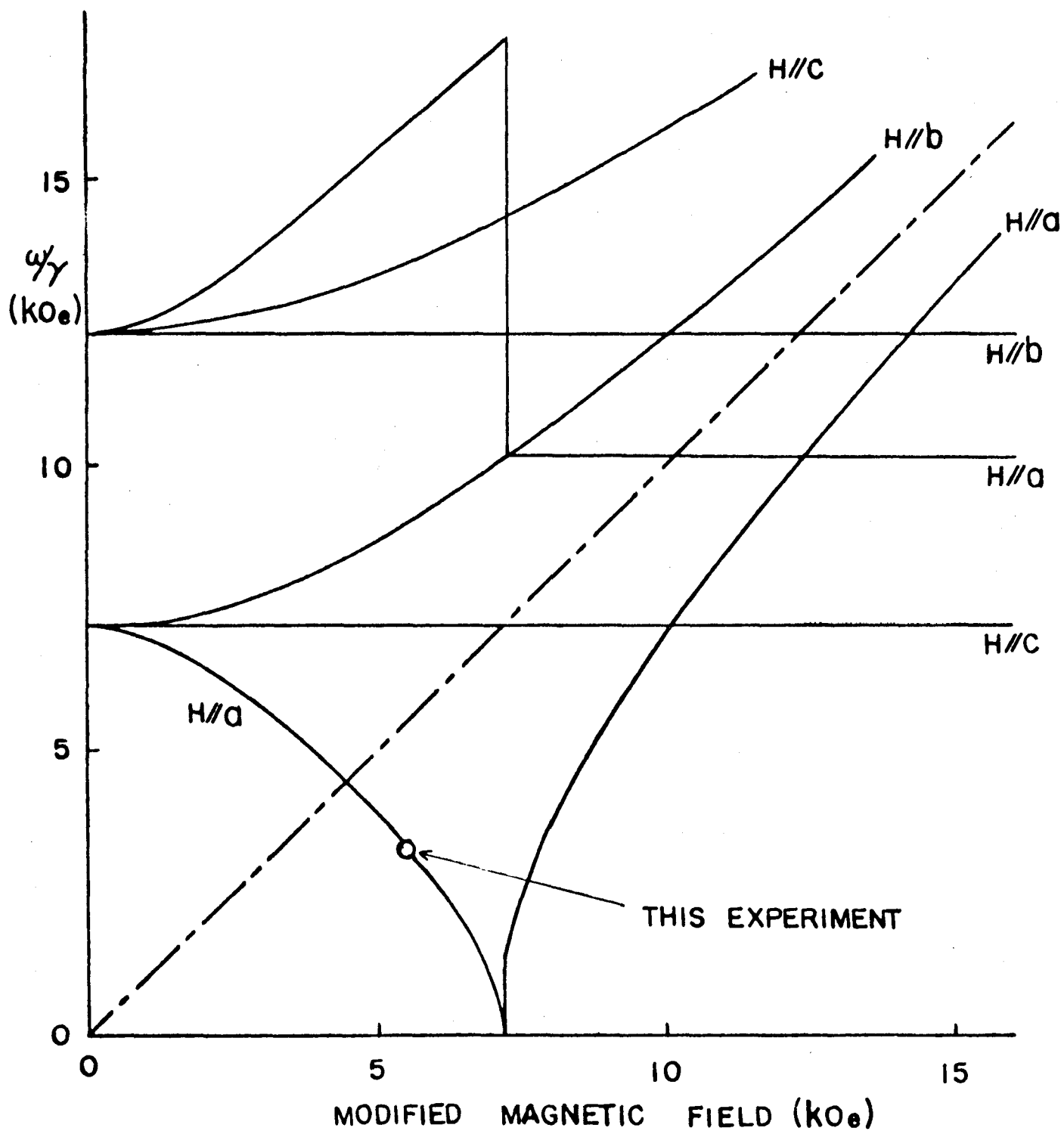


Fig.8 Frequency-field diagram of the resonance points
in $\text{CuCl}_2 \cdot 2\text{H}_2\text{O}$ at 0°K .

shifts toward higher field with increasing microwave magnetic field h_1 . Moreover it also shifts toward higher field as the pulse is broader (Fig.9). But the resonance point observed at the start of the pulse (MP_1) does not shift with the microwave power change. As the origin of the shift, two possible mechanisms are considered: the first is the shift induced by a large angle precession of the magnetization under high power excitation and the second is the shift due to a rise in spin temperature. Now we consider first the shift due to the increase of the precession angle. When the higher k spin-waves are excited the individual spins in the same sub-lattice are tilted. In this case, the calculation of the shift is rather complicated because the shift will depend on the number of excited $k=0$ and $k \neq 0$ magnons with a k -dependent factor. It may be allowed to estimate the limit of the shift on the basis of molecular field approximation, though this approximation is inaccurate to calculate the shift. The equation of motion of the two sub-lattice magnetizations is

$$\frac{1}{\gamma} \frac{d}{dt} M^{\pm} = M^{\pm} \times (H + H_e^{\pm} + H_a^{\pm}), \quad (5)$$

where M^{\pm} is the magnetization of the + and - sublattice, H , H_e , and H_a represent the external magnetic field, the exchange field and the anisotropy field, respectively. Following Nagamiya and Yosida's procedure, we define

$$M = M^+ + M^-, \quad M' = M^+ - M^-. \quad (6)$$

Now an exchange field is given by

$$H_e^+ = -AM^- - \Gamma M^+, \quad (7)$$

and anisotropy field is

$$H_a^{\pm} = \left(-\frac{K_1 M_x^{\pm}}{M_0^2}, -\frac{K_2 M_y^{\pm}}{M_0^2}, 0 \right), \quad (8)$$

where x , y , and z axes correspond to the b , c , and a axes of the

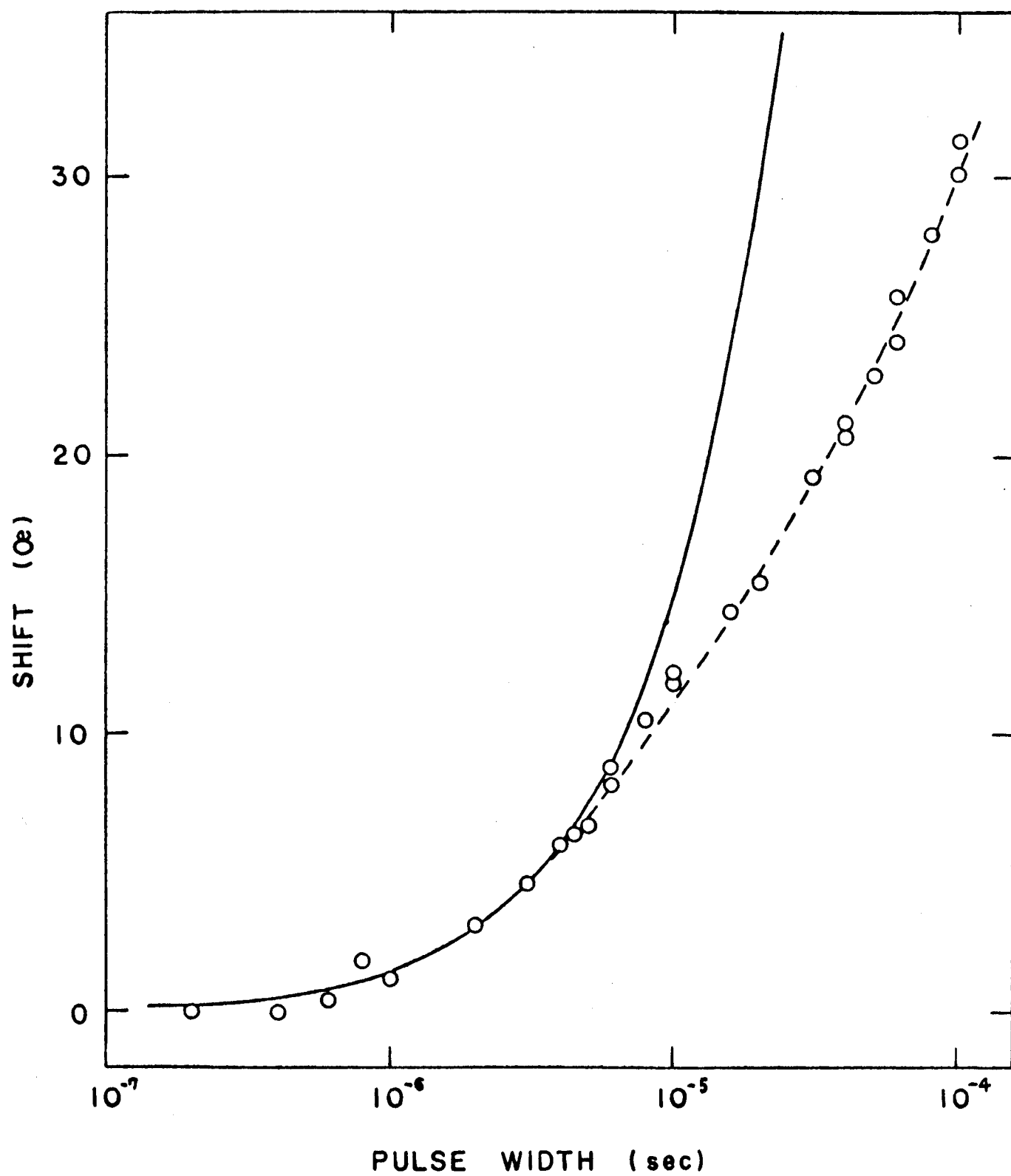


Fig.9 Resonance field shifts at the end of pulse with varying pulse width.

$\text{CuCl}_2 \cdot 2\text{H}_2\text{O}$ crystal, respectively, and M_0 is the sublattice magnetization. When the applied field is smaller than H_c and is parallel to the z-axis, the equation of motion of M and M' can be written as follows:

$$\left. \begin{aligned} \frac{1}{\gamma} \frac{dM_x}{dt} &= \left(H + \frac{K_2 M_z}{2M_0^2} \right) M_y + \frac{K_2 M'_z}{2M_0^2} M'_y, \\ \frac{1}{\gamma} \frac{dM_y}{dt} &= - \left(H + \frac{K_1 M_z}{2M_0^2} \right) M_x - \frac{K_1 M'_z}{2M_0^2} M'_x, \\ \frac{1}{\gamma} \frac{dM_z}{dt} &= 0, \end{aligned} \right\} \quad (9)$$

$$\left. \begin{aligned} \frac{1}{\gamma} \frac{dM'_x}{dt} &= (H - AM_z + \frac{K_2 M_z}{2M_0^2}) M'_y + (AM'_z + \frac{K_2 M'_z}{2M_0^2}) M_y, \\ \frac{1}{\gamma} \frac{dM'_y}{dt} &= -(AM_z + \frac{K_1 M'_z}{2M_0^2}) M'_x - (H - AM_z + \frac{K_1 M_z}{2M_0^2}) M'_x, \\ \frac{1}{\gamma} \frac{dM'_z}{dt} &= 0. \end{aligned} \right\} \quad (10)$$

Noticing the first order correction of the large angle precession in ^{addition} to the Nagamiya-Yosida's procedure, the secular determinant of the resonance frequency is given by

$$\begin{vmatrix} -\frac{i\omega}{\gamma} & H & 0 & \frac{K_2 M'_z}{2M_0^2} \\ -H & -\frac{i\omega}{\gamma} & -\frac{K_1 M'_z}{2M_0^2} & 0 \\ 0 & AM'_z & -\frac{i\omega}{\gamma} & H - AM_z \\ -AM'_z & 0 & -H + AM_z & -\frac{i\omega}{\gamma} \end{vmatrix} = 0. \quad (11)$$

In Nagamiya-Yosida's theory, terms such as AM'_z and AM_z are simply written by $2AM_0$ and 0 at $0^\circ K$, respectively. Under high rf-field, however, changes of M_z and M'_z cannot be neglected. We therefore have

$$\left(\frac{\omega}{\gamma}\right)^4 - \left(\frac{\omega}{\gamma}\right)^2 \left\{ C_1' + C_2' + H^2 + (H-AM_z)^2 \right\} + H^2 (H-AM_z)^2 - H(H-AM_z)(C_1' + C_2') + C_1' C_2' = 0, \quad (12)$$

where

$$C_1' = AK_1 \frac{M_z^2}{2M_0^2}, \quad C_2' = AK_2 \frac{M_z'^2}{2M_0^2}. \quad (13)$$

The terms $(AM_z)^2$ in the coefficient of $(\omega/\gamma)^2$ in Eq.(12) can be neglected in the case of $H \gg AM_z$. This simplifies the calculation and we have

$$H(H-AM_z) = \frac{1}{2} \left[2\left(\frac{\omega}{\gamma}\right)^2 + C_1' + C_2' \pm \left\{ 8(C_1' + C_2')\left(\frac{\omega}{\gamma}\right)^2 + (C_1' - C_2')^2 \right\}^{1/2} \right]. \quad (14)$$

For $\omega = 9.0$ kMc/sec, H was numerically calculated with varying the ratio M_z/M_0 from 10^{-5} to 10^{-2} at $T = 0^\circ K$. The estimation of M'_z was made as follows: M'_z can be calculated from M_z and θ_2/θ_1 where θ_1 is the angle between M^+ and the z-axis and θ_2 is the angle between M^- and the z-axis (Fig.1). The ratio of θ_2 to θ_1 is given by

$$\frac{\theta_2}{\theta_1} \simeq 1 + \left(\frac{2H_a}{H_e}\right)^{1/2}. \quad (15)$$

Since the anisotropy energy of $CuCl_2 \cdot 2H_2O$ has an orthorhombic symmetry, the precession of the magnetization is not circular but elliptic. For simplicity, however, we use an effective H_a estimated as follows: In the uniaxial case at $0^\circ K$, Eq.(2)

is given by

$$\left(\frac{\omega}{\gamma}\right)^2 = (H - \sqrt{C})^2. \quad (16)$$

Experimental values of $\omega = 9.0$ kMc/sec and $H = 5500$ Oe. (which is the modified field^V by $H = (g/2)H_{\text{experiment}}$ given) were substituted in Eq.(16) and we obtain the effective C to be

$$C = 2H_a H_e = 75.9 \times 10^6 \text{ Oe}^2. \quad (17)$$

This value and $H_e = 1.16 \times 10^5$ Oe, which is estimated by Joenk,³¹⁾ is substituted in Eq.(15) and we have

$$\frac{\theta_2}{\theta_1} = 1.075. \quad (18)$$

Fig.10 shows the resonance field H with varying the ratio M_z/M_0 . H shifts toward lower field with increasing M_z/M_0 up to $(M_z/M_0) = 4 \times 10^{-3}$. A shift less than 2 Oe is expected by the magnetization $M_z = (4 \pm 3) \times 10^{-4} M_0$ which was induced by the antiferromagnetic resonance at 1.4°K (the practical estimation of M_z will be discussed later). Therefore the shift of the resonance induced by the change of the precession angle is negligible. Next we consider the shift due to the temperature rise of the spin system. A temperature dependence of the resonance field was measured by Ubbink²⁴⁾ and was well explained by Eq.(2). More detailed measurements of the temperature dependence of the resonance field in the temperature range $1.4 < T < 2.0^\circ\text{K}$ were done and the result is shown in Fig.11. In this temperature region the resonance position gradually shifts toward higher field with increasing temperature.

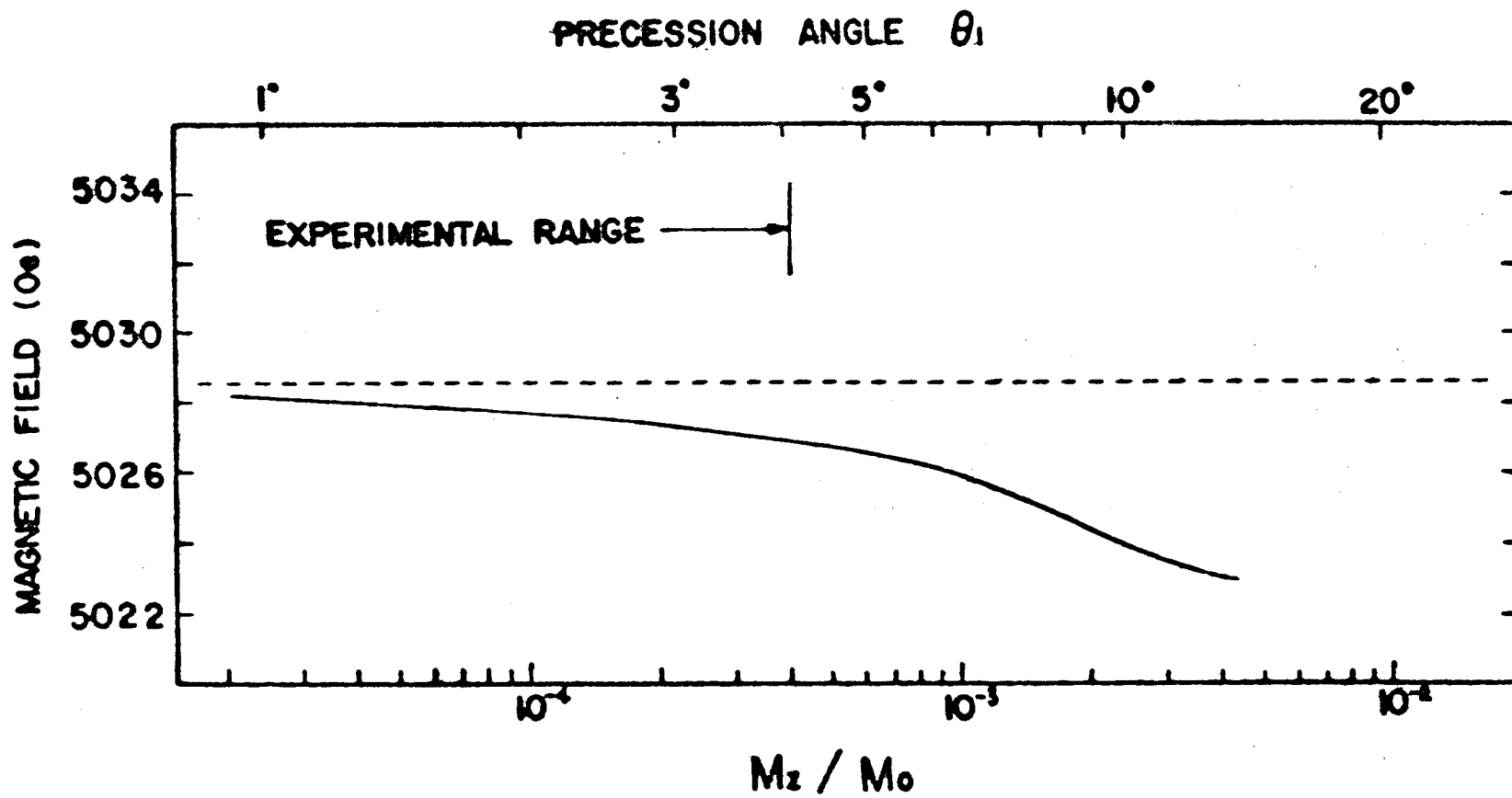


Fig. 10 Calculation of the resonance field shift when the precession angle increases.

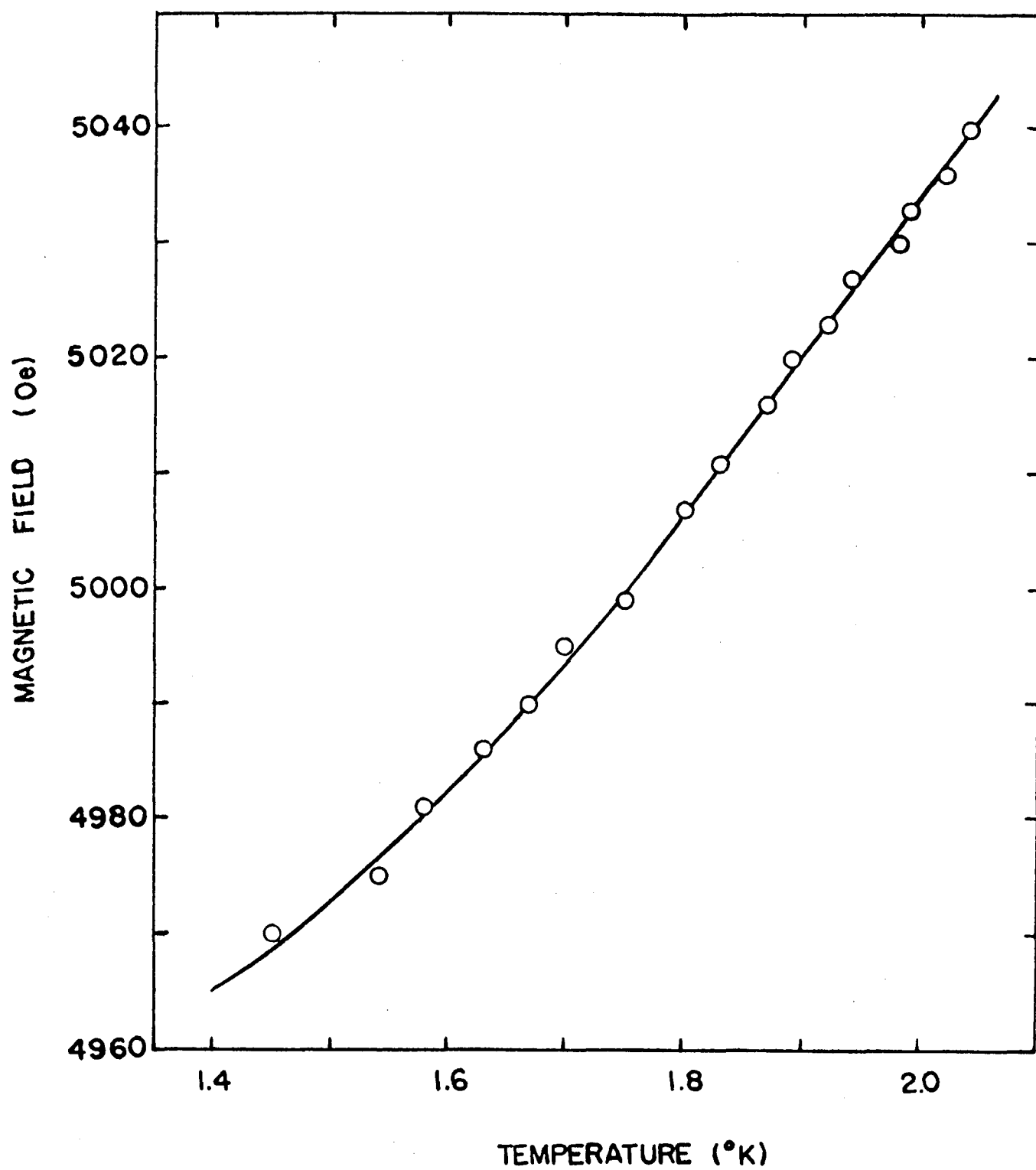
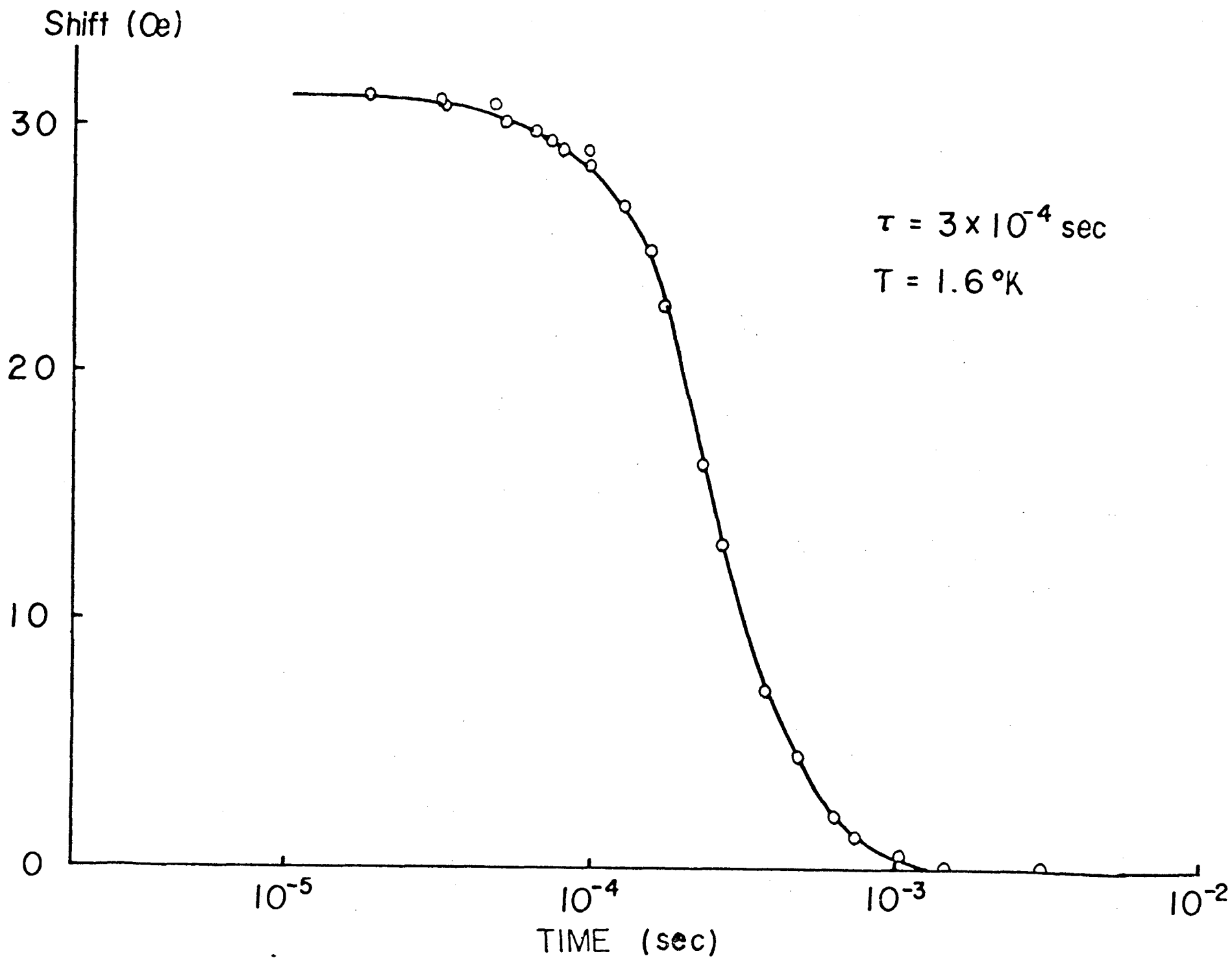


Fig.11 Temperature dependence of the resonance field
at 9.1 kMc/sec.

Therefore one can estimate the spin temperature under resonance by using the data shown in Fig.11. An example of the heating shift is shown in Fig.9. Open circles in the figure represent the observed shift as a function of pulse duration time when a pulsed microwave (160 mW peak power) was applied. The solid curve is drawn under an assumption that there is no heat transfer from the crystal to He bath, namely, the assumption that all energies given by the microwave should stay in the crystal. Apparent deviations between the solid curve and observed points are seen nearly above 10^{-5} sec. This means that the energy flow relaxation time from lattice to bath is of the order of 1×10^{-5} sec. Detailed estimation of the lattice-bath relaxation time will be given later. Similar relaxation effect was observed just after the cutoff of a microwave. The resonance position returns gradually toward the low power position. A transient recovery of the resonance position was monitored by applying another low power microwave. A result at $T=1.6^{\circ}\text{K}$ is given in Fig.12 where thermal recovery occurs with a characteristic time of 3×10^{-4} sec. It is noticed that the relaxation time obtained at the beginning of a pulse is about $1/30$ smaller than observed at the thermal recovery process. Detailed discussions concerning with this discrepancy will be given later.

The resonance line shape under saturation was investigated using a continuous high power microwave. The line shape becomes asymmetric when a microwave power increases because the resonance shift due to heating makes the line shape complex.

Fig.12 A transient recovery of the resonance position after the cutoff of a microwave.



When a magnetic field approaches to the resonance field from lower field, the field for the resonance shifts to higher field but the absorption stops abruptly at a certain magnetic field. This shift terminates in a discrete jump of the resonance line to the low power position. When the field approaches to the resonance from the higher field, the resonance line is pulled up slightly as is shown in Fig.13. Such a hysteresis effect is easily explained by the shift due to heating. A low frequency unstable oscillation was also observed when a magnetic field was in this hysteresis region with the oscillation frequency of about 1 kc/sec. The origin of this oscillation can be explained by the following mechanism: Under a strong rf-field, the sample absorbs microwaves and then the resonance shifts to the higher field. Accordingly the off-resonant condition occurs just after the microwave absorption and so the spin system becomes cold. Then the first resonance condition without shift realizes again. This push-pull effect was actually observed at high microwave power levels.

b) Linewidth.

In many antiferromagnetic crystals, temperature independent residual linewidths were measured and it is believed that the residual linewidth of an antiferromagnetic resonance originates from lattice distortions or crystal imperfections. In fact, when a sample of $\text{CuCl}_2 \cdot 2\text{H}_2\text{O}$ was first immersed in liquid helium the linewidth is the narrowest. The linewidth of the same sample becomes broader and the line shape becomes complex with repetition^{of} the process of cooling and heating. It may

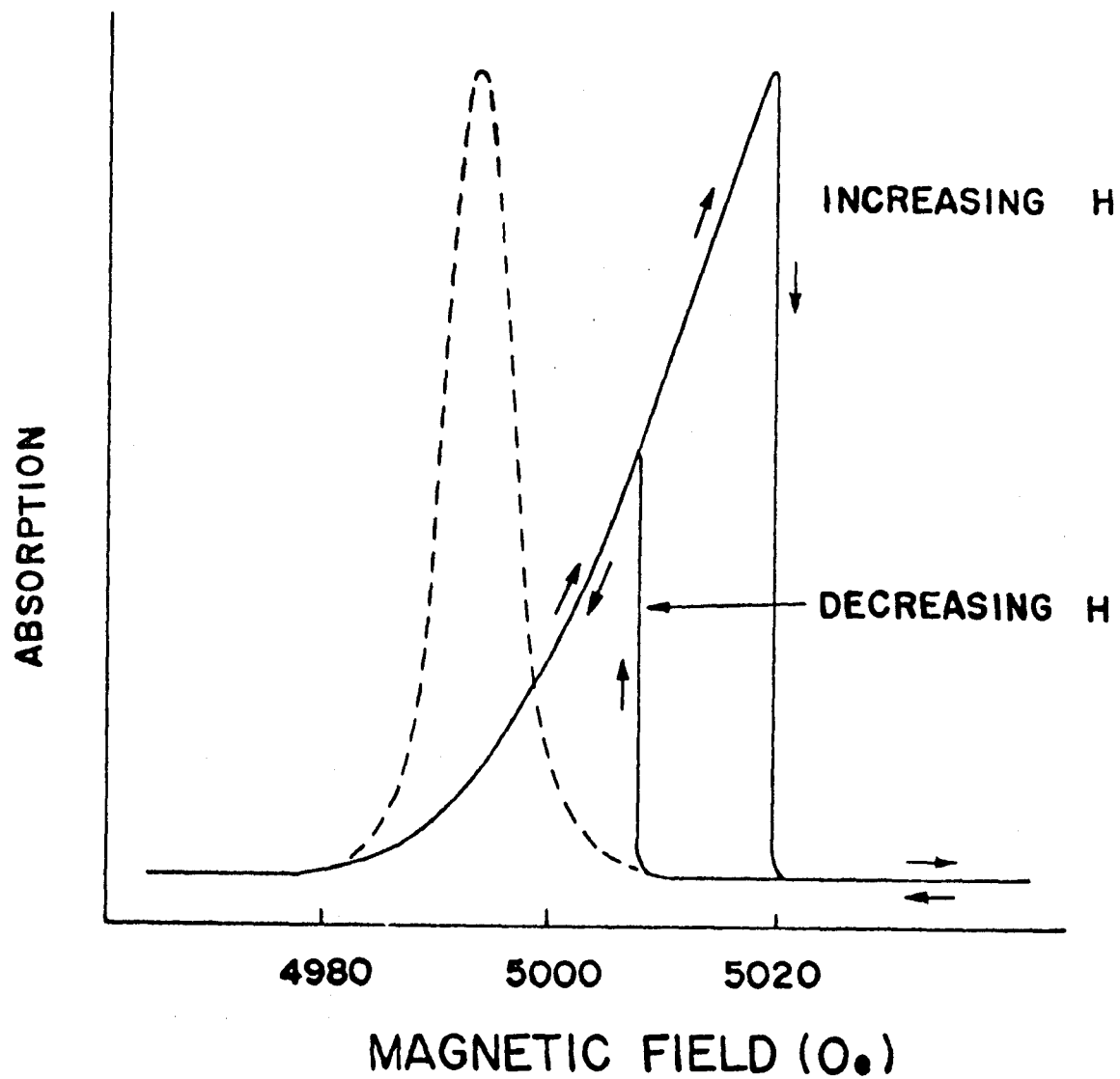


Fig.13 Resonance line shape by a continuous high power microwave.

be said that the linewidth is broadened on account of many invisible cracks caused by rapid cooling. A temperature dependence of antiferromagnetic resonance linewidth in $\text{CuCl}_2 \cdot 2\text{H}_2\text{O}$ was measured in the temperature range $1.4 < T < 2.6^\circ\text{K}$. The observed narrowest linewidth is 7 Oe at 1.4°K which is smaller than that of the same compound measured by Gerritsen et al.¹⁾ and is smaller than that of any other antiferromagnet, for instance, 300 Oe of MnF_2 ²⁾ and 20 Oe of $\text{CuF}_2 \cdot 2\text{H}_2\text{O}$.³⁾ Since the measurements were made at a constant frequency rather than a constant field, a correction factor $(1/\gamma)(d\omega/dH)$ should be multiplied to the experimental values. This correction factor can be obtained from Eq.(2) and it is shown in Fig.14. The reduced full half-linewidths are given in Fig.15. After subtracting the residual width, the results were compared with a T^2 curve. As is shown in Fig.15, the temperature dependence of linewidth cannot be represented by T^2 throughout the temperature range of the experiment. The temperature range of this experiment satisfies the condition of $kT > \hbar\omega_L$ and $\hbar\omega_h$ is comparable to kT and there are no corresponding theory to explain the result. Theoretical work on antiferromagnetic resonance linewidth has been done by several authors but the results are in disagreement with one another. The temperature dependence of linewidth is proportional to T^1 by Urushadze,⁹⁾ T^2 by Kawasaki⁵⁾ and Tani⁷⁾ or T^3 by Harris⁶⁾ in the temperature range of $kT/g\mu_B \gg (2H_e H_a)^{1/2}$. We cannot measure the linewidth at high power because the line shape is distorted as shown in Fig.13. It is well known that a full half-linewidth ΔH between the points of half maximum absorption may be considered as a measure of the antiferromagnetic relaxation. Now we define T_2 as the corresponding relaxation time, namely,

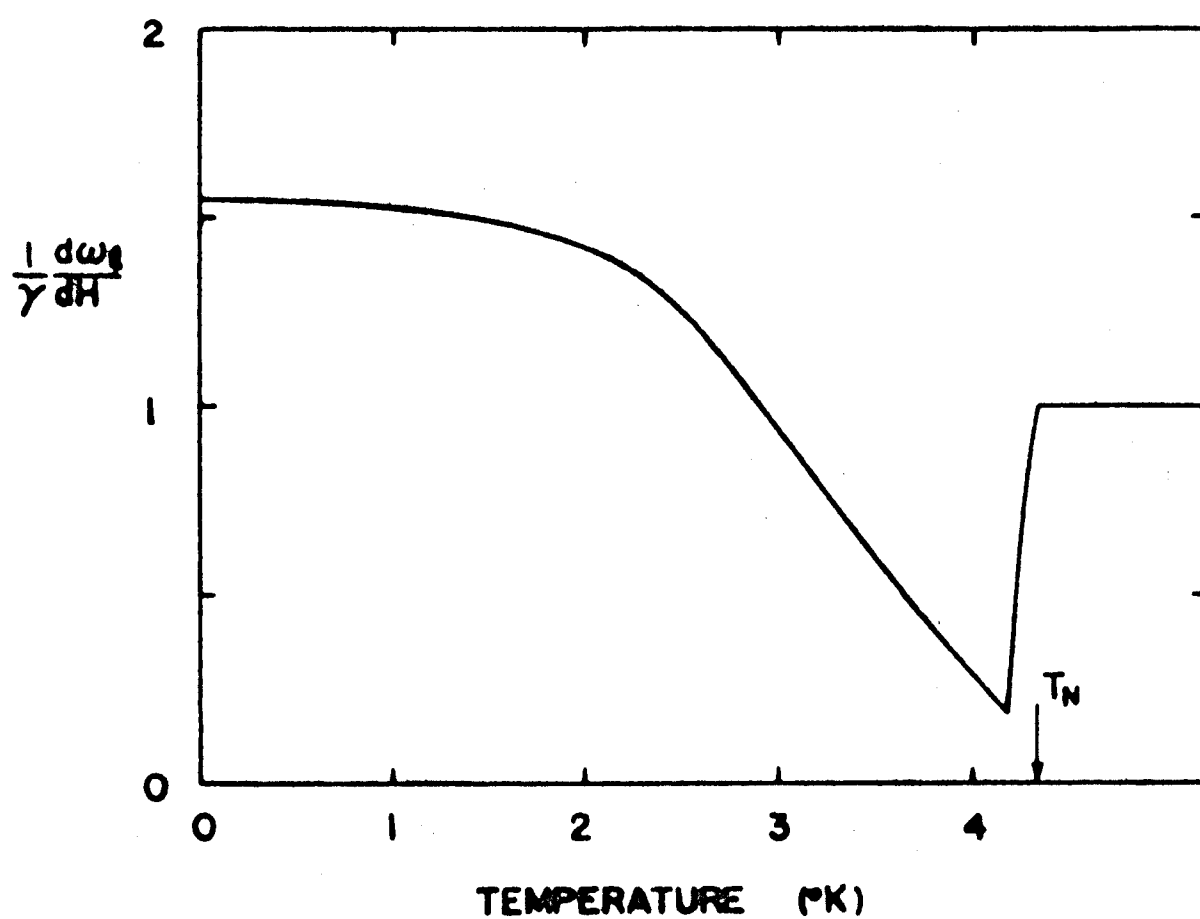


Fig.14 Temperature dependence of $\frac{1}{\gamma} \frac{d\omega_f}{dH}$.

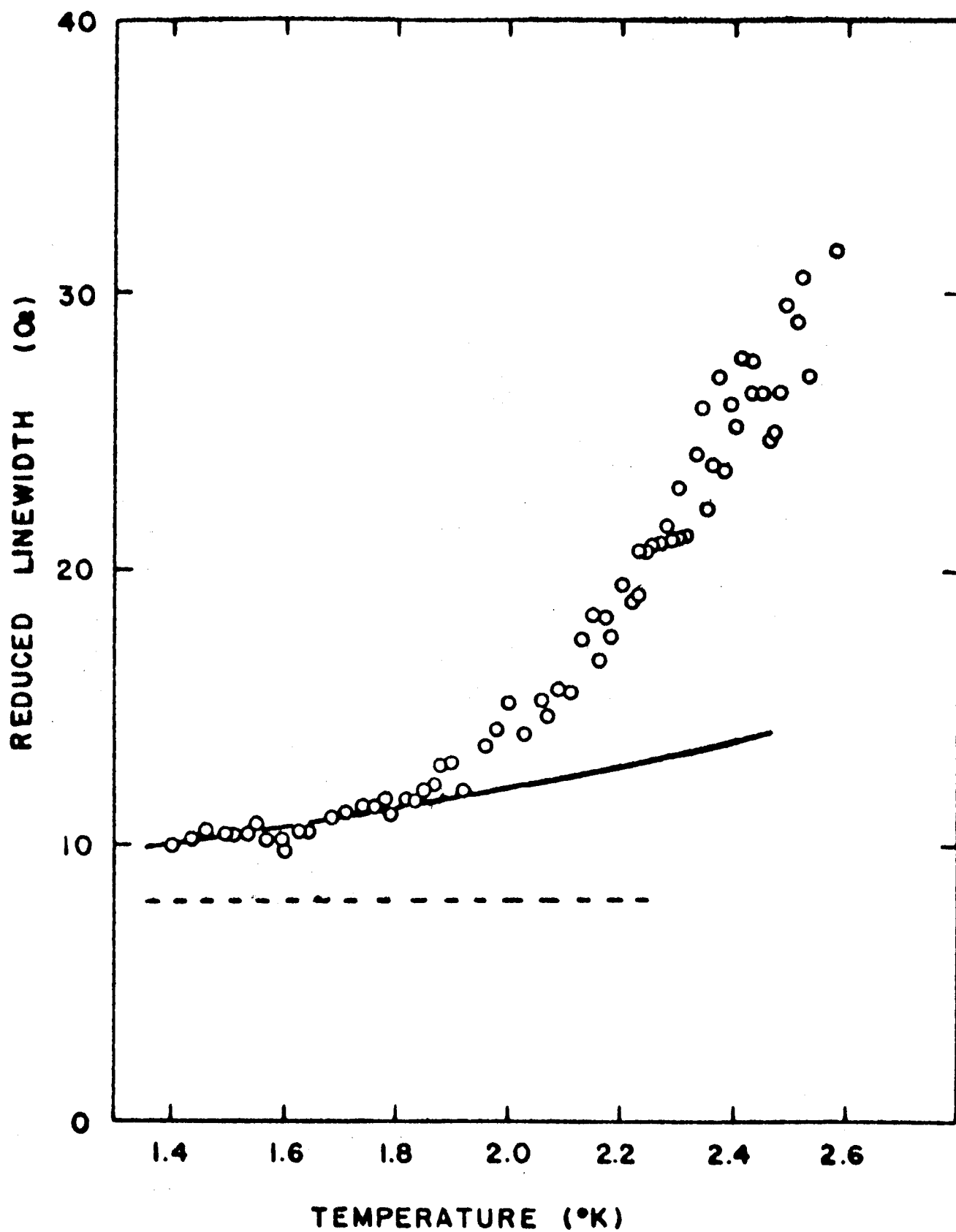


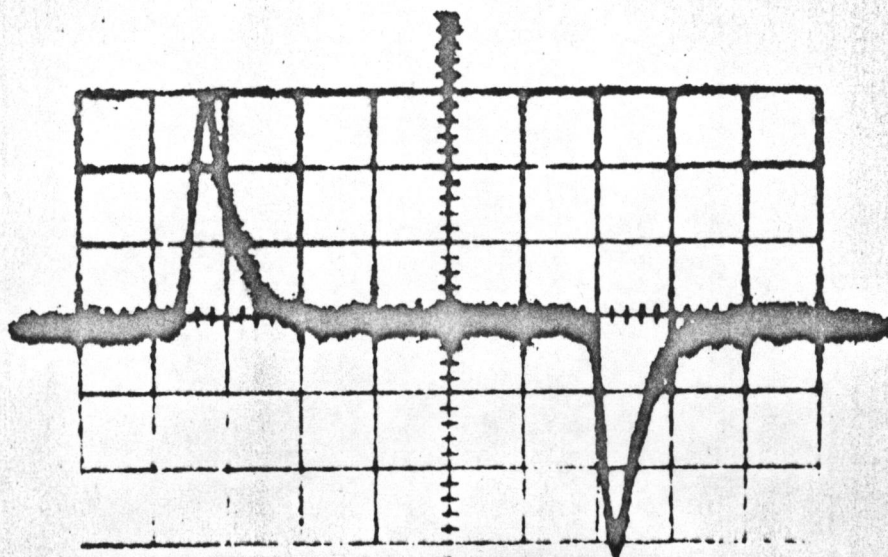
Fig. 15 Temperature dependence of antiferromagnetic resonance linewidth. Solid curve shows $\Delta H = T^2 + 8$.

$$T_2 = \frac{2}{\gamma \Delta H}, \quad (19)$$

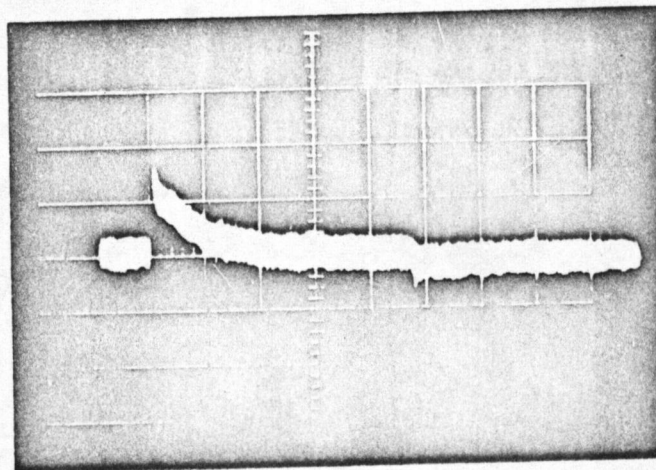
The reduced linewidth of 10 Oe (true width is 7 Oe) at 1.4°K corresponds with $T_2 = 6 \times 10^{-8}$ sec.

c) Measurement^{of} M_z and the relaxation times.

Considering carefully the facts discussed in (a) and (b), the differential magnetization induced in the pick-up coil were investigated in detail. As a conclusion, it was found that there are two characteristic relaxation times describing the z-magnetization change induced by the antiferromagnetic resonance. Fig.16 shows these two relaxation phenomena. In Fig.16(a),^{the} rise and decay curves of dM_z/dt at resonance are illustrated with rapid sweep. The relaxation time calculated from this figure is of the order of $10^{-7} \sim 10^{-8}$ sec. between 1.4 and 2.0°K and is called hereafter as T_{1a} . One more slow relaxation time called T_{1b} is shown in Fig.16(b), which is of the order of $10^{-3} \sim 10^{-5}$ sec in the same temperature region. Now let us discuss first the rapid relaxation time T_{1a} . The measurements of T_{1a} were made in the temperature range from 2.0 to 1.4°K and an observed temperature dependence of T_{1a} is shown in Fig.17. It is found that T_{1a} is shorter than 3×10^{-8} sec above 2.0°K and that the data in the range $1.4 < T < 2.0^\circ\text{K}$ are well described by an empirical expression $T_{1a} = (1.1 \pm 0.1) \times 10^{-6} T^{-(5 \pm 0.5) / 32}$. An interesting fact is that T_{1a} observed at MP_i (T_{1a}^i) is not equal to that at MP_f (T_{1a}^f). Usually T_{1a}^f is shorter than that of T_{1a}^i and depends on the



(a)



(b)

Fig.16 Induced signals by the change of M_z . (a) Signal of relaxation time T_{1a} . (1×10^{-7} sec per division.) (b) Signal of relaxation time T_{1b} and signal of T_{1a} is also seen both at the beginning and the end of pulse. (2×10^{-5} sec per division)

$T_1 \times 10^8 \text{ (sec)}$

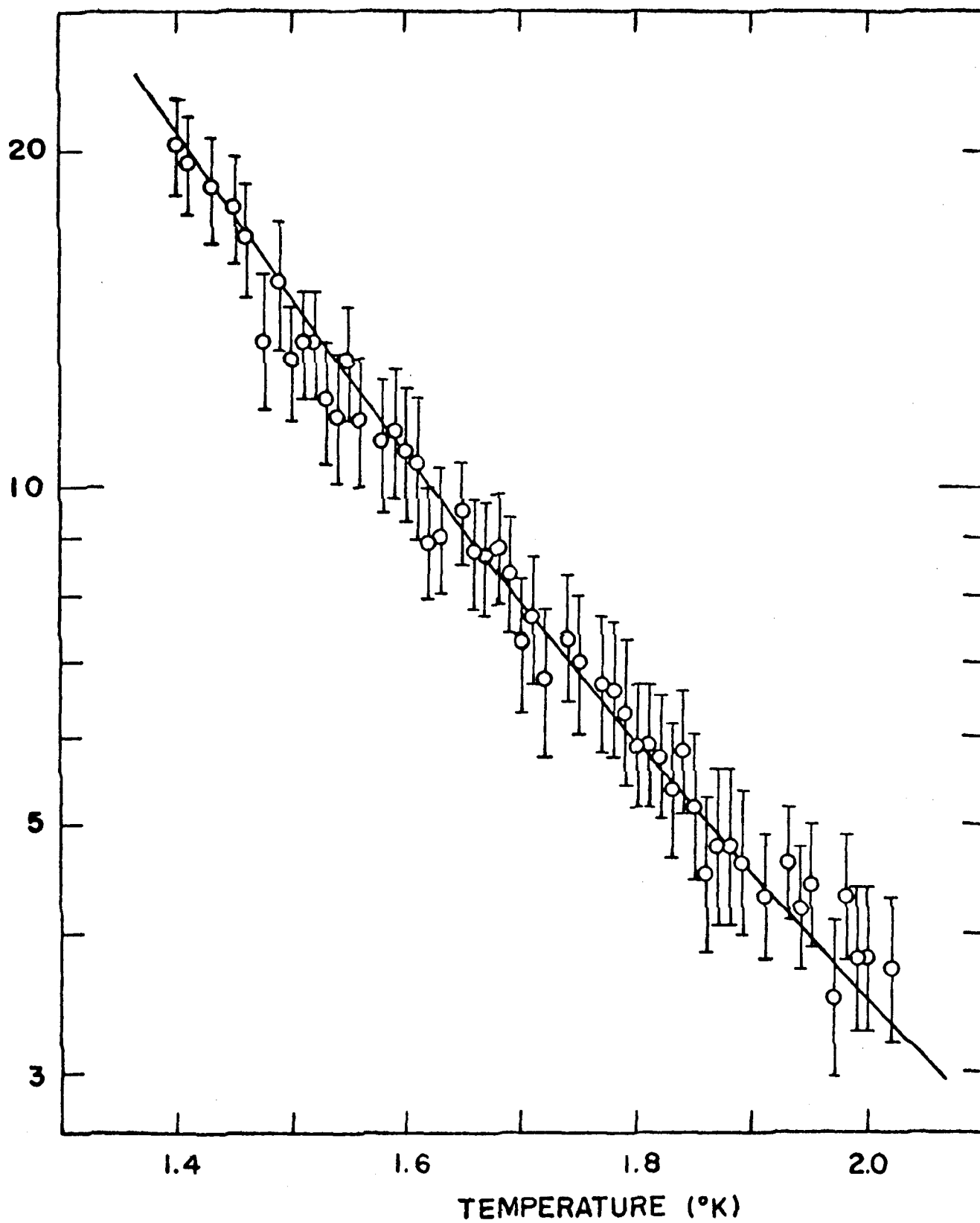


Fig.17 Temperature dependence of T_{1a} .

pulse width and microwave power (Fig.18 and 19). As is easily understood, this shortening effect comes from heating up of the specimen. To verify this, two methods of estimating the temperature of the specimen are compared. In Fig.20, temperatures estimated from the resonance shift and change of the relaxation time T_{1a}^f are shown. The agreement between both estimates is satisfactory.

Angular dependences of T_{1a} in the ab and ac planes were measured and shown in Fig.21 and 22. When H is applied along the a-axis, T_{1a} is the largest. This can be qualitatively understood as follows: When H is parallel to the z-axis, the motion of ^{the} spins is of the simple form so that the possibility to include non-diagonal elements concerning their relaxation is smaller than ⁱⁿ the case where H ^{is} inclined from the z-axis.

Now let us consider the total magnetization change under resonance. Under a 160 mW pulsed microwave at 1.4°K, dM_z/dt becomes zero after about 10^{-7} sec. Calibrating the induced flux due to dM_z/dt , the induced magnetization M_z at this time was determined as

$$\frac{M_z}{M_0} = 4 \times 10^{-4} \quad (20)$$

where M_0 is the sublattice magnetization. If we assume that there are no change of the sublattice moments, a schematic view of the precession can be drawn as ⁱⁿ Fig.23(a) and the induced moment is given by Fig.23(b). The condition of $2T_{1a} = T_2$ is required in order to conserve the magnetization. but the transverse relaxation time T_2 calculated from the

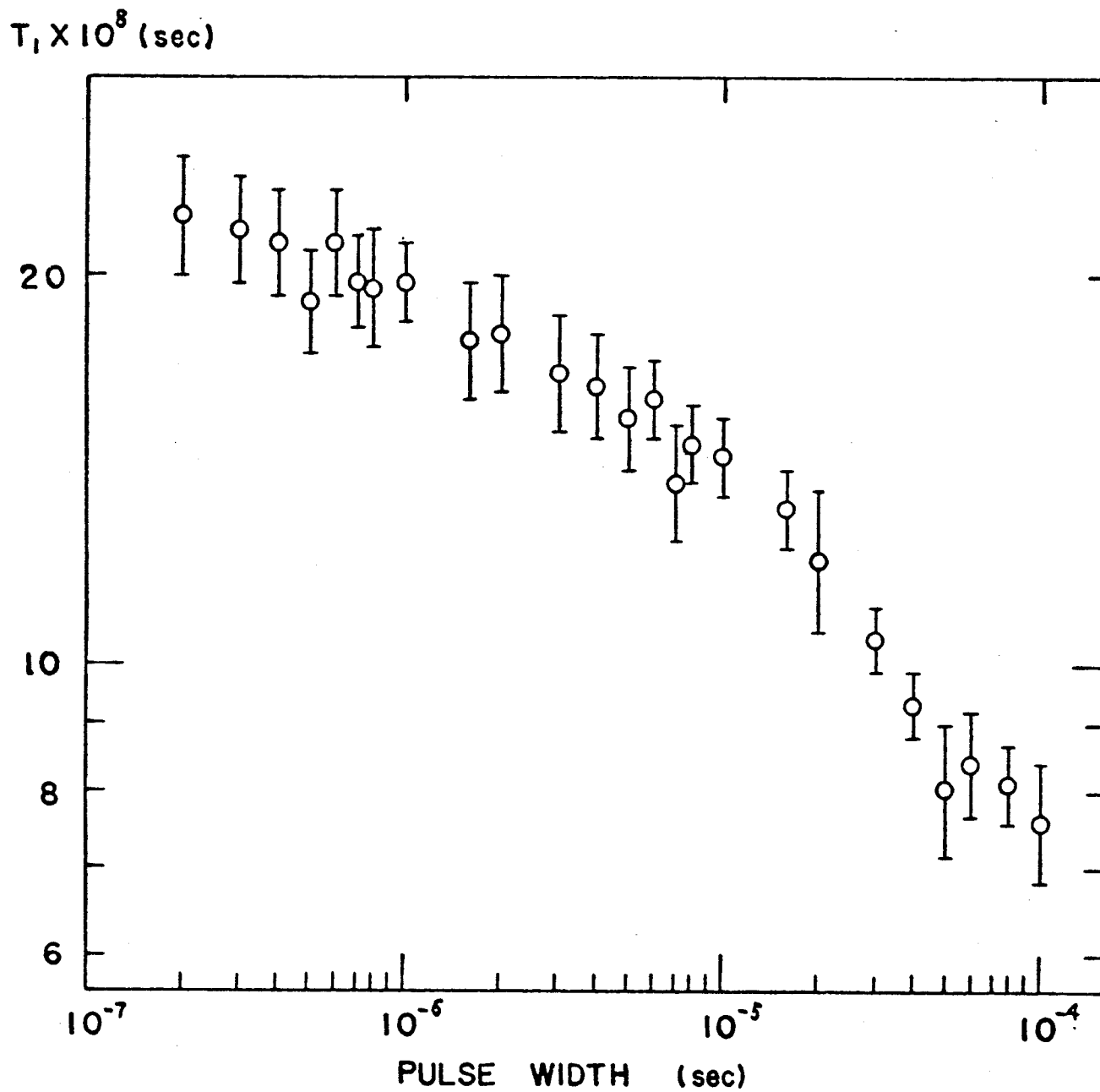


Fig. 18 An example of T_{1a}^f observed at the end of the pulse at 1.4°K (160 mW peak power).

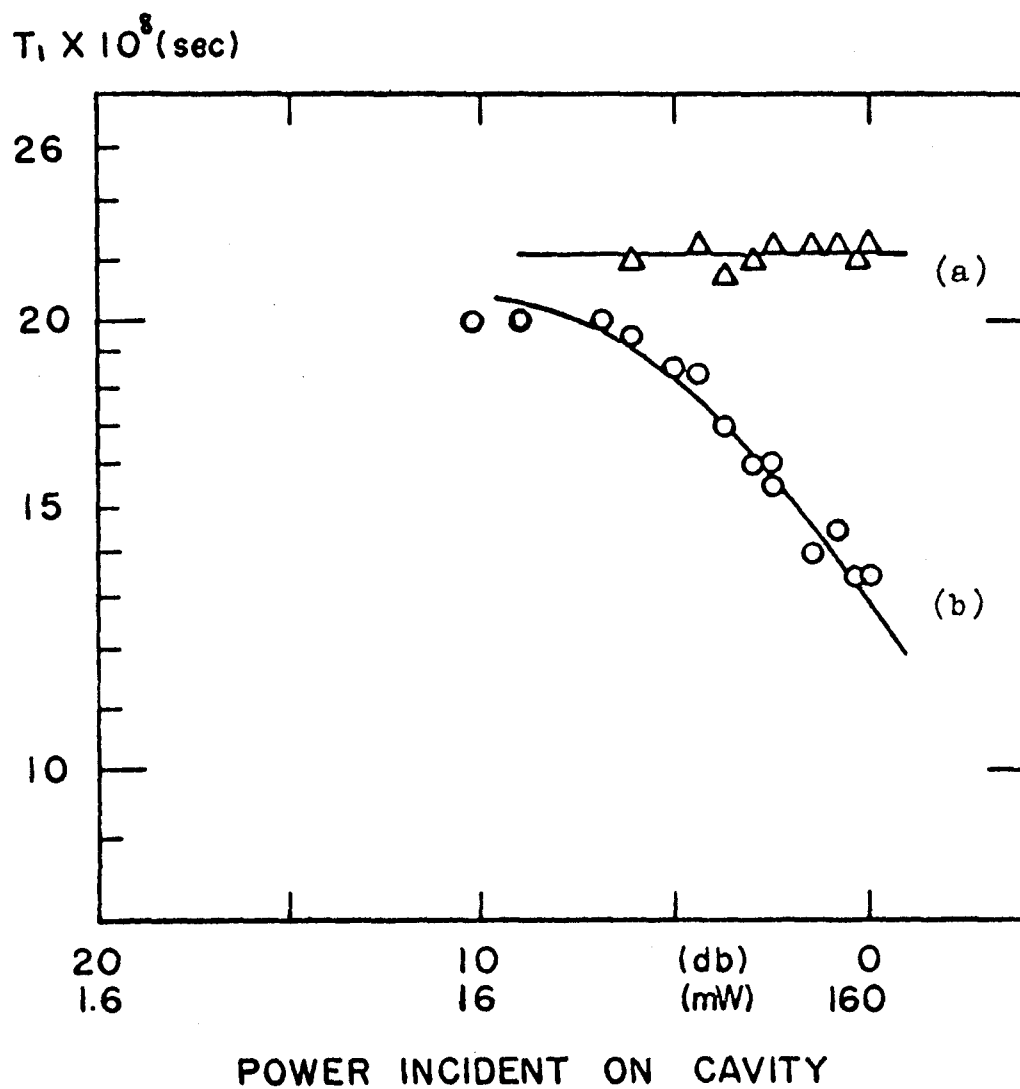


Fig.19 Power dependence of T_{1a}^f at the end of the pulse.
Pulse widths are 1 μsec (a) and 10 μsec (b).

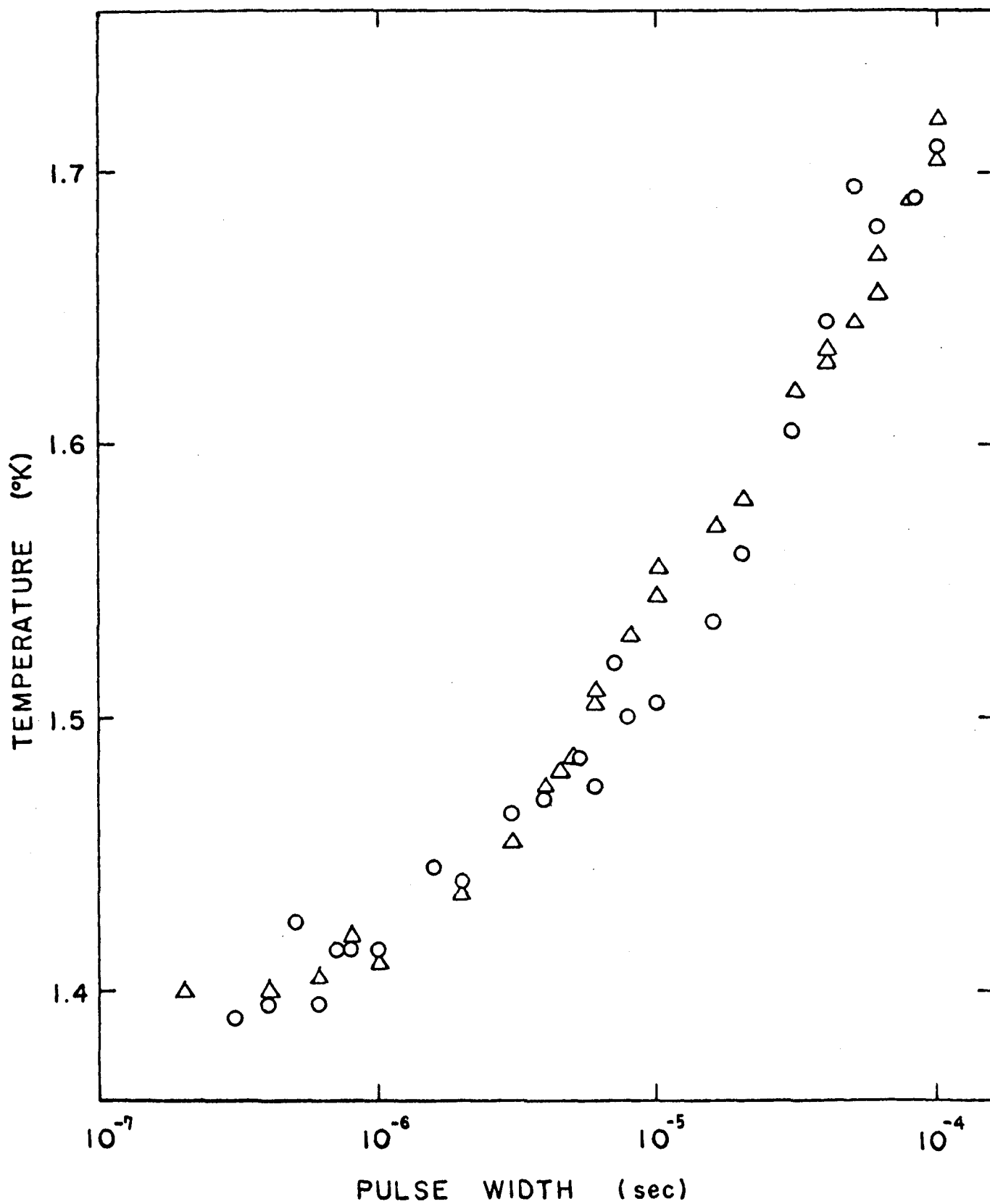


Fig.20 Temperature at the end of the pulse introduced by both resonance position(O) and $T_{1a}^f(\Delta)$.

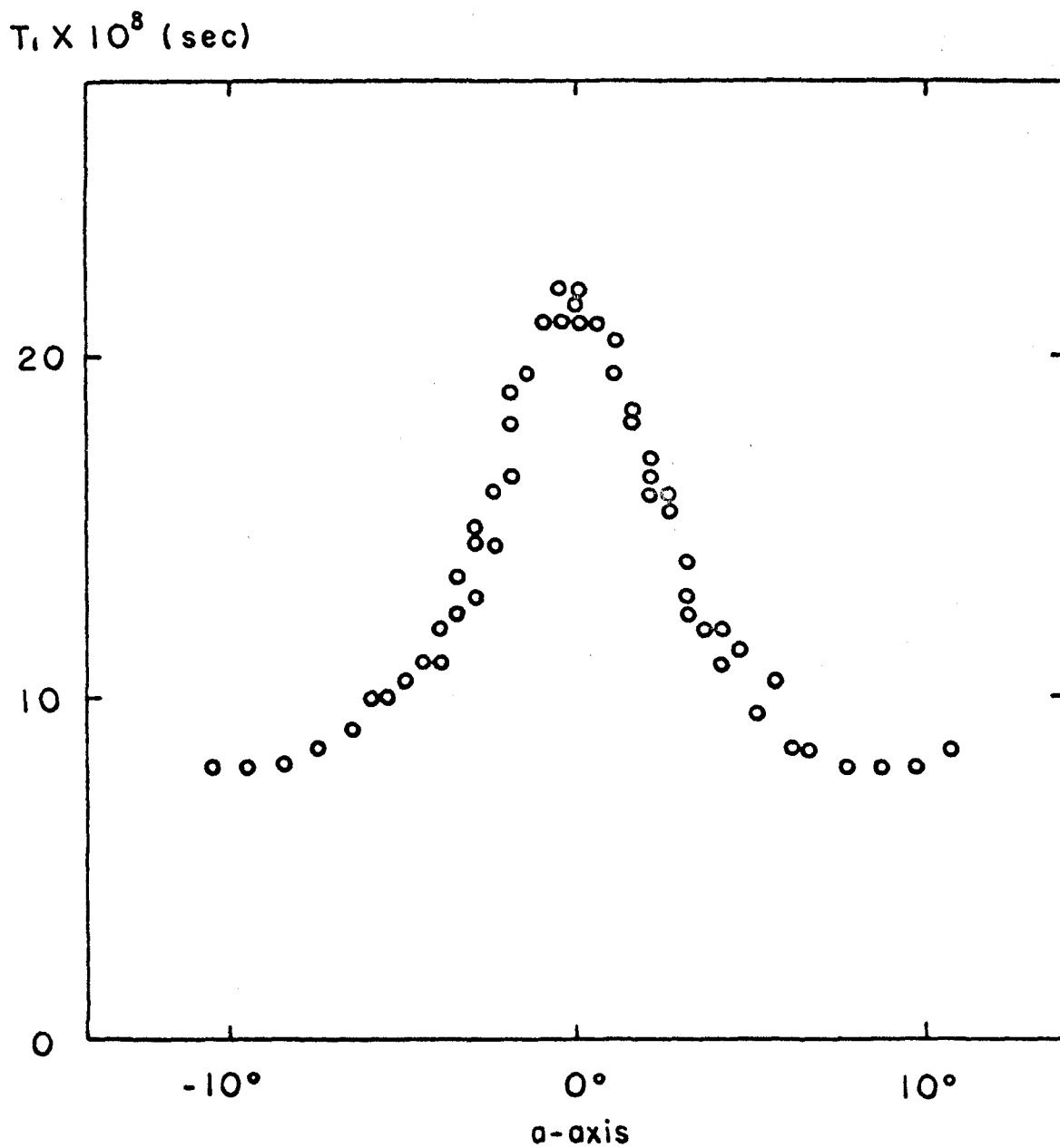


Fig.21 Angular dependence of T_{1a} in the ab -plane at 1.4°K .

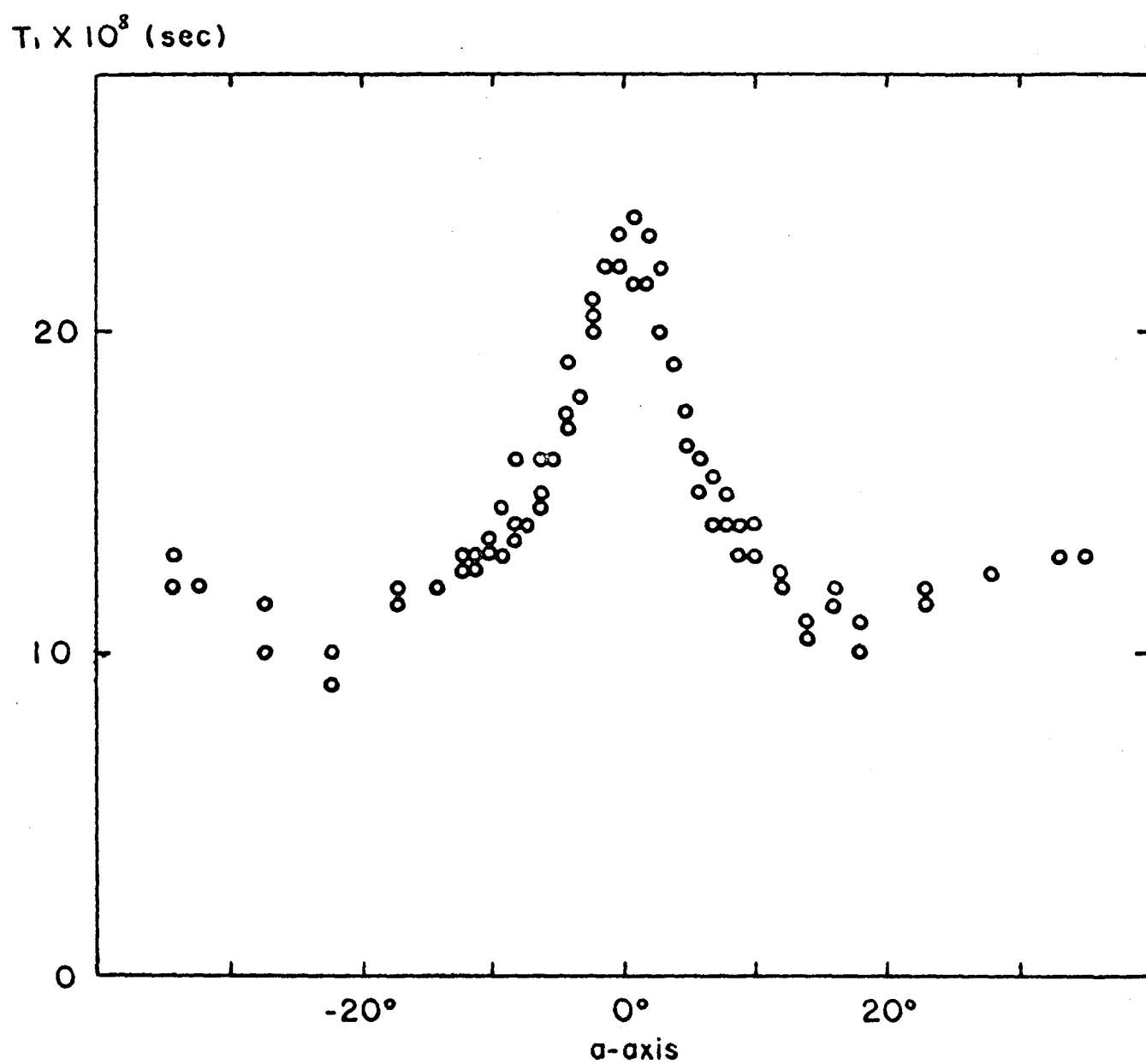


Fig.22 Angular dependence of T_{1a} in the ac -plane at 1.4°K .

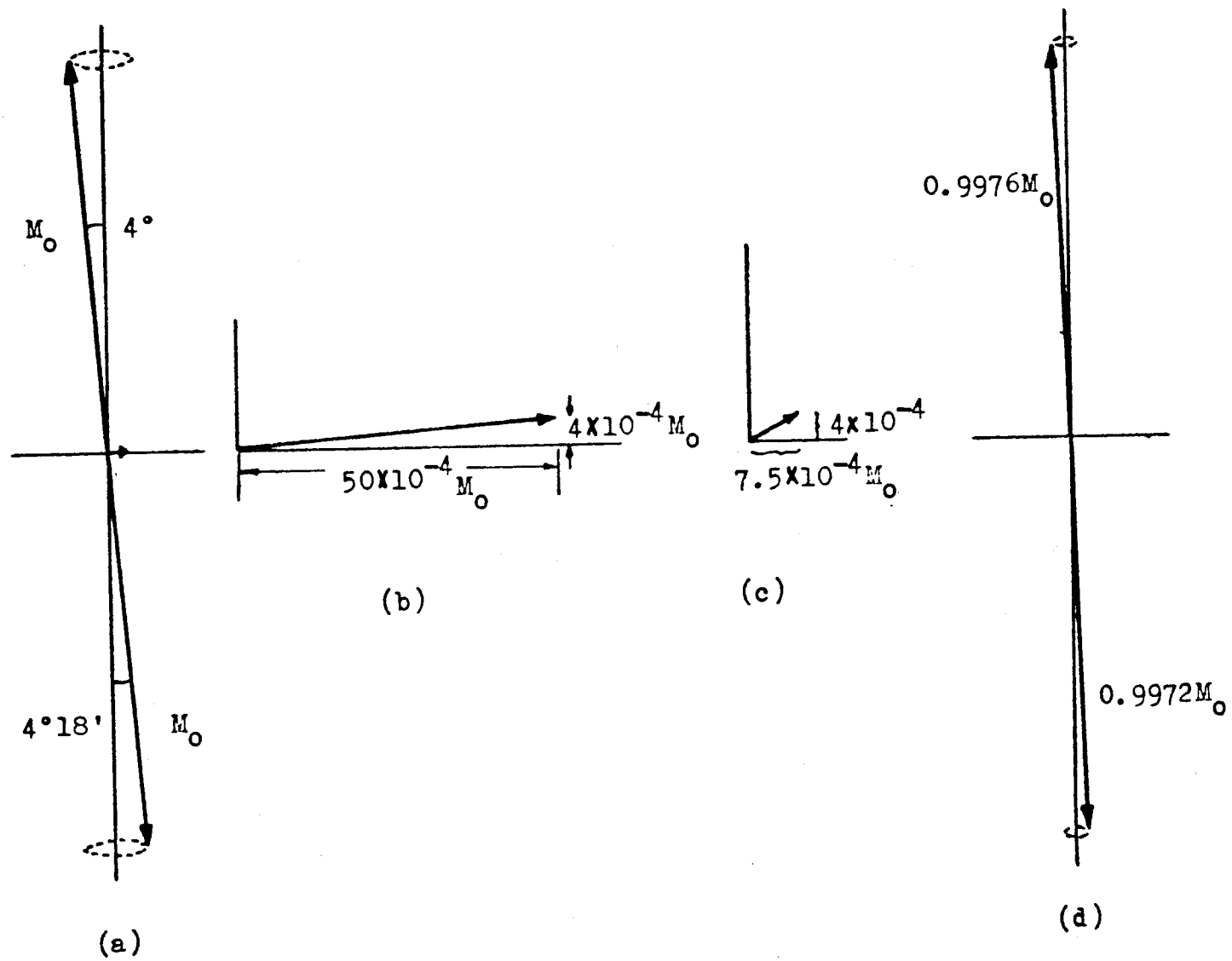


Fig. 23 Antiferromagnetic resonance and relaxation in $\text{CuCl}_2 \cdot 2\text{H}_2\text{O}$ at 1.4°K under 160 mW .

linewidth is 6×10^{-8} sec and $T_{1a} = 2 \times 10^{-7}$ sec at 1.4°K . Therefore the transverse component of the magnetization $M_{x,y}$ in Fig.23(b) is overestimated by a factor of $2T_{1a}/T_2$ and so $M_{x,y}$ should be as given in Fig.23(c). The corresponding scheme of the sublattice magnetizations are represented by Fig.23(d). Thus the behavior of the induced magnetization in $\text{CuCl}_2\cdot 2\text{H}_2\text{O}$ at the initial stage of the high power microwave pulse can be visualized easily. The heating up effect of the spin system was also investigated by varying the microwave power and pulse width. One of the results is shown in Fig.24 and M_z at the end of a pulse is given in Fig.25 as a function of pulse width.

Next we discuss another relaxation time T_{1b} which is very long compared with T_{1a} . Because of the long relaxation time we used a pick-up coil of 0.5 mH which was placed near the slit outside the cavity. An example of the experimental data is shown by a photograph given in Fig.16(b). An interesting fact is that this relaxation time depends on the condition of liquid helium bath. Fig.26 shows the temperature dependences of T_{1b} especially near T_λ which means the transition temperature of liquid helium from He I to He II. T_{1b} is constant in the ab-plane as is shown in Fig.27. Considering these facts, the relaxation time T_{1b} is attributed to the lattice-bath relaxation time in $\text{CuCl}_2\cdot 2\text{H}_2\text{O}$. Power dependences of T_{1b} were also investigated (Fig.28) but other complex change of the relaxation is not understood yet.

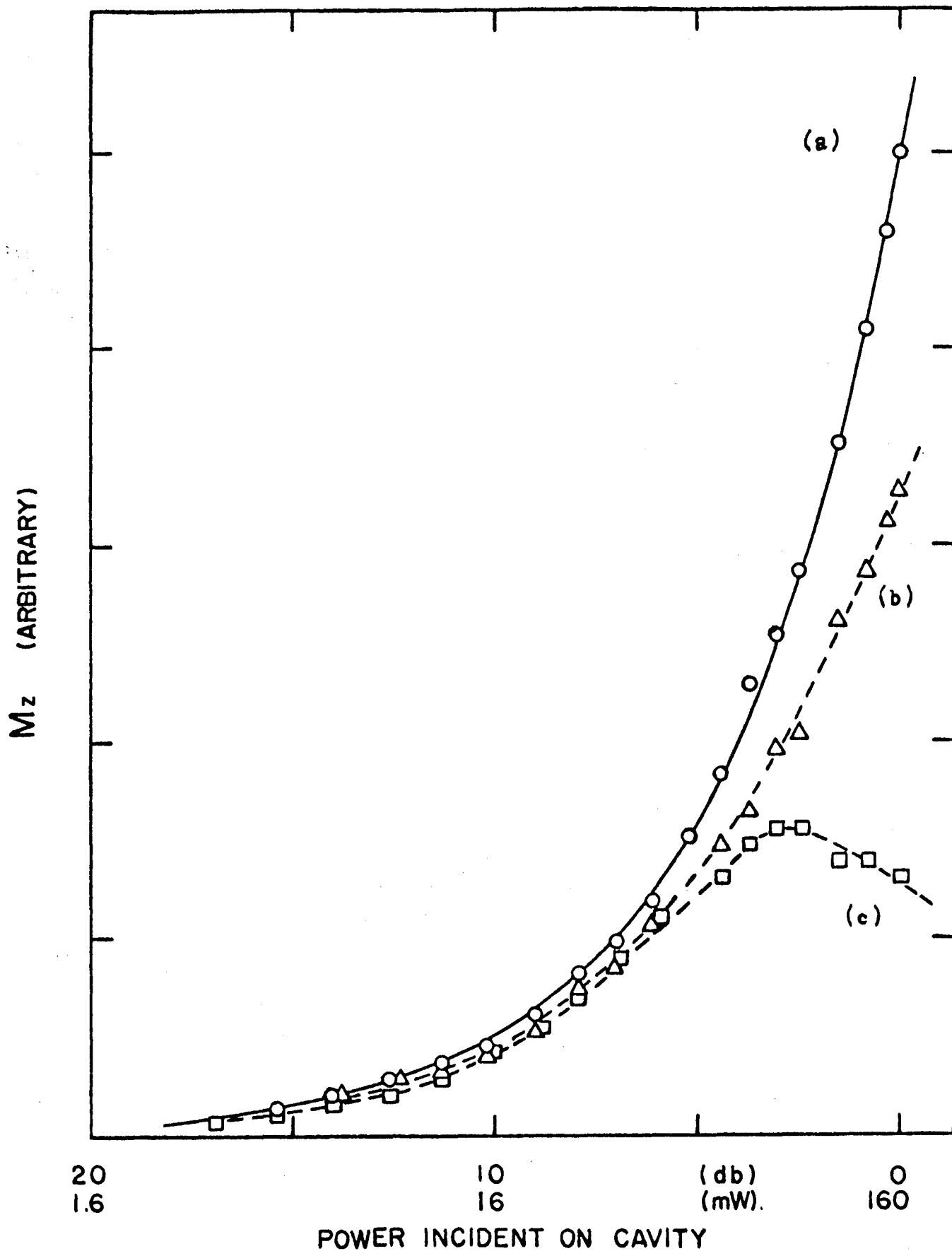


Fig.24 Power dependences of M_z at 1.4°K. (a) M_z at the beginning of the pulse, (b) at the end of 1 μ sec pulse, and (c) at the end of 10 μ sec pulse.

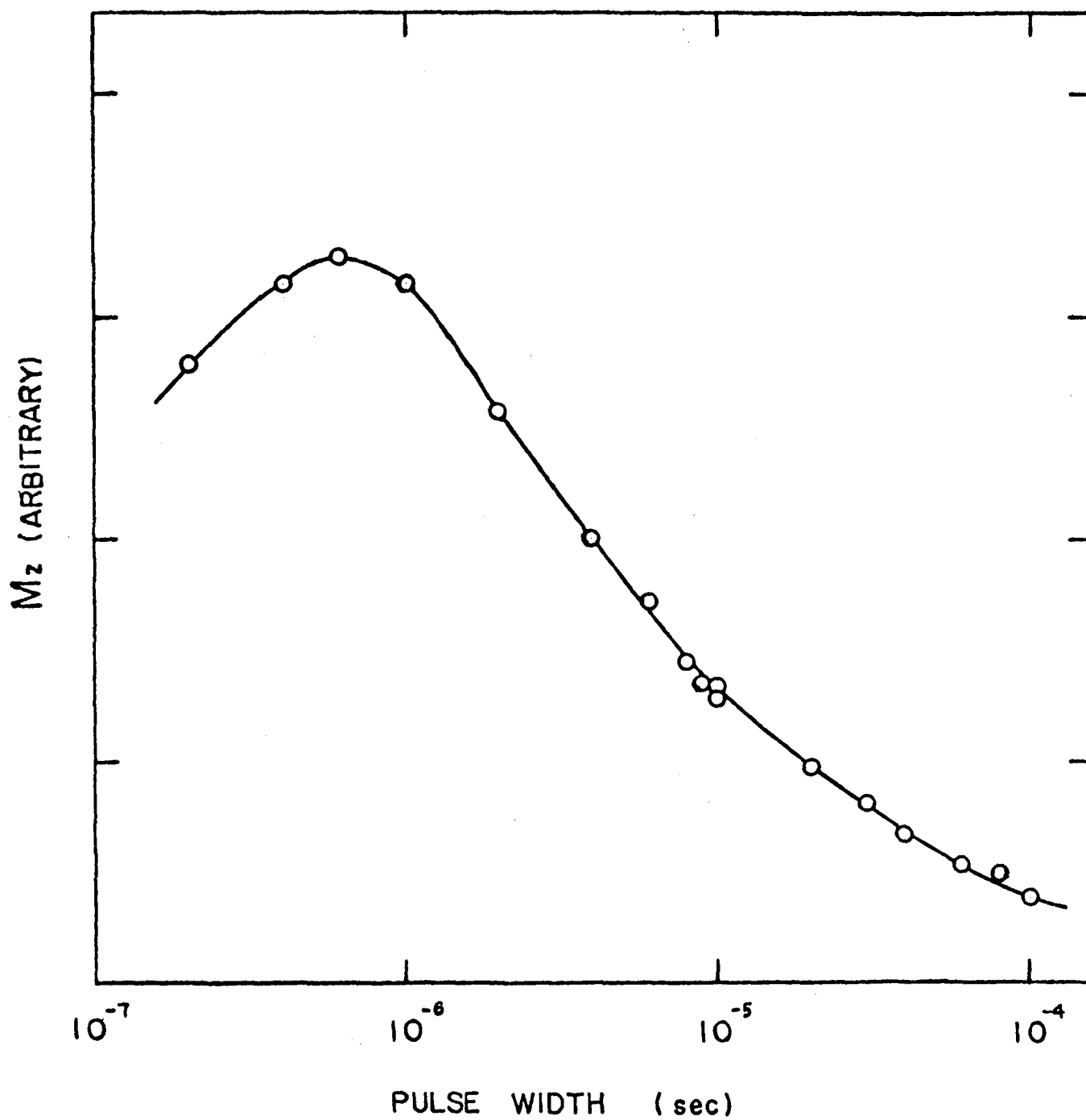


Fig.25 M_z at the end of the pulse as a function of pulse width (160 mW peak power).

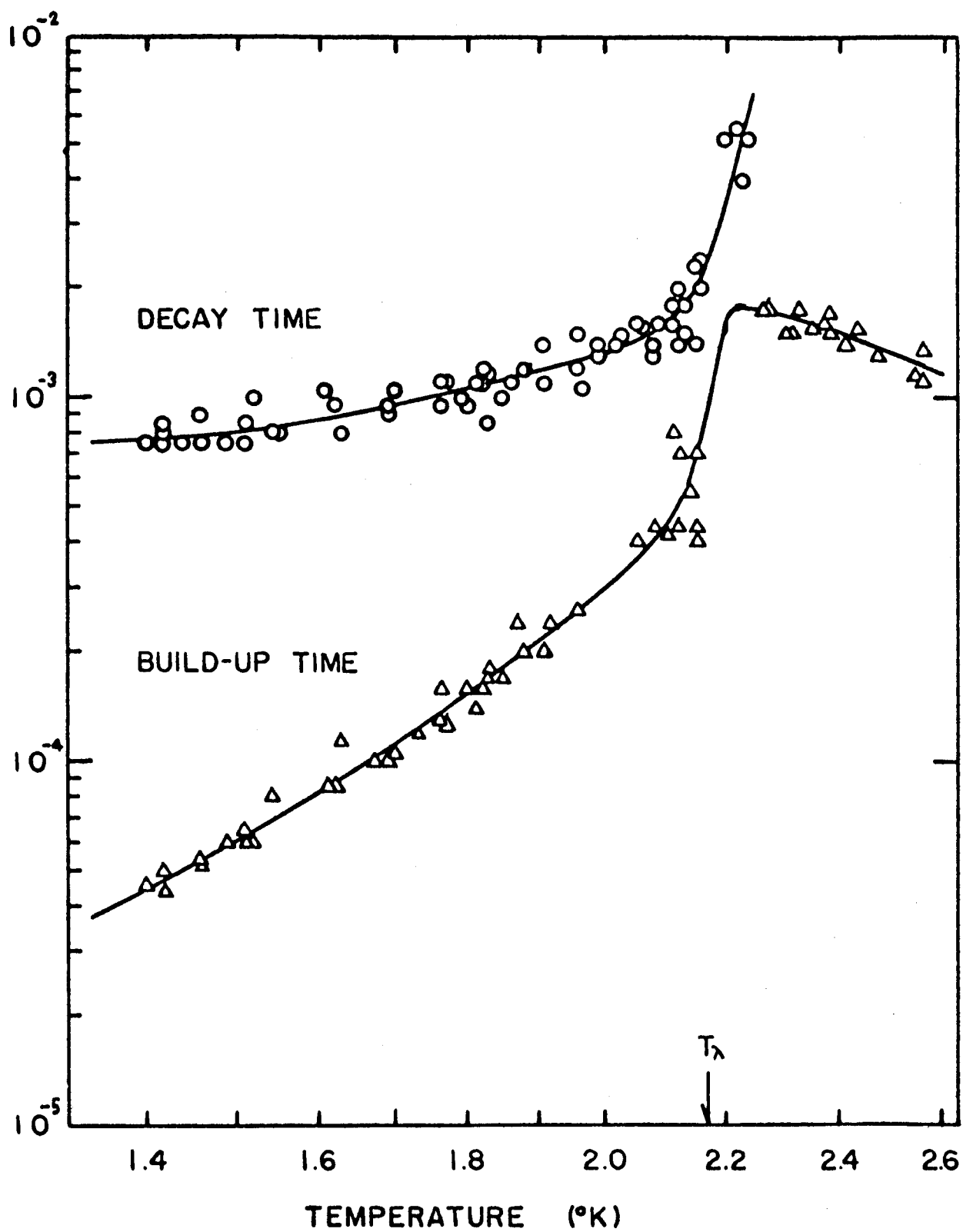


Fig.26 Temperature dependences of T_{1b} .

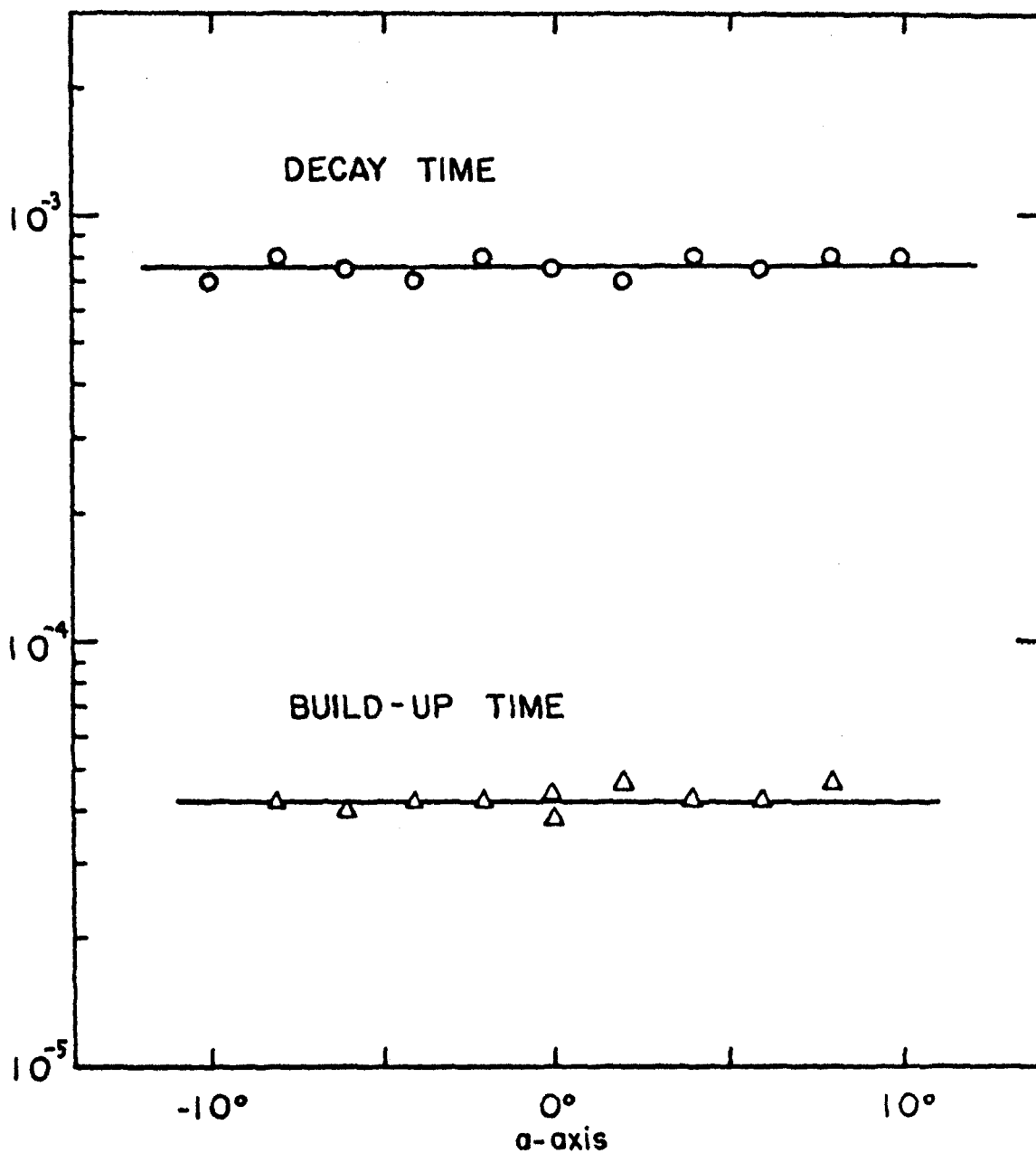


Fig.27 Angular dependences of T_{1b} in the ab-plane at 1.4°K.

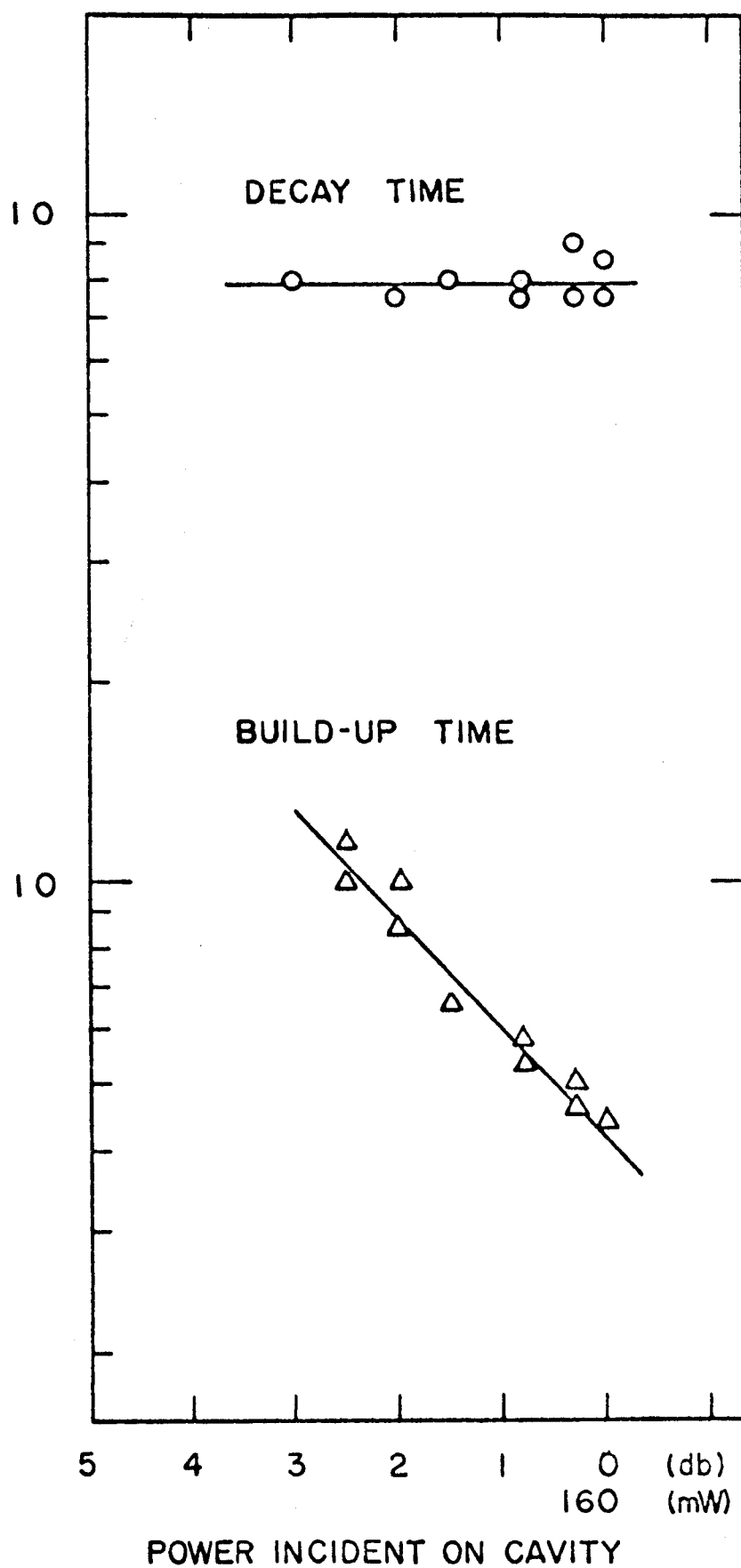


Fig.28 Power dependence of T_{1b} at 1.4°K.

d) Measurements of χ'' and $M_{x,y}$.

Heeger¹³⁾ found that the imaginary part of rf susceptibility χ'' at antiferromagnetic resonance in KMnF_3 declined with increasing h_1 and ^{he} pointed out that this effect might be due to the onset of spin-wave instability analogous to that for a ferromagnet, though he did not observe M_z induced by antiferromagnetic resonance. His argument is as follows: When the uniform mode reaches a critical amplitude, the effect of the nonlinear terms will cause an exponential growth of the degenerate higher spin-wave which is degenerate in energy with the uniform mode. This exponential growth acts as a loss of the uniform mode and holds ^{of the latter} the amplitude \wedge fixed at the critical value. Therefore, an increase in rf field does not yield a corresponding increase in transverse moment, since the higher k spin-waves ^{no} have \wedge net transverse moment. This produces an apparent saturation of the uniform mode rf susceptibility in a magnetic resonance experiment. In consequence, Heeger derived the critical rf field h_c for the onset of instability to be

$$h_c = 4 \Delta H_0 (\gamma \Delta H_K / \omega_0)^{1/2}, \quad (21)$$

where ΔH_0 and ΔH_K are, respectively, the uniform mode and spin-wave linewidths, and ω_0 is the antiferromagnetic resonance frequency.

We observed power dependences of χ'' of antiferromagnetic resonance in $\text{CuCl}_2 \cdot 2\text{H}_2\text{O}$ using microwave pulses of various widths at 1.4°K as is shown in Fig.29. χ'' at resonance

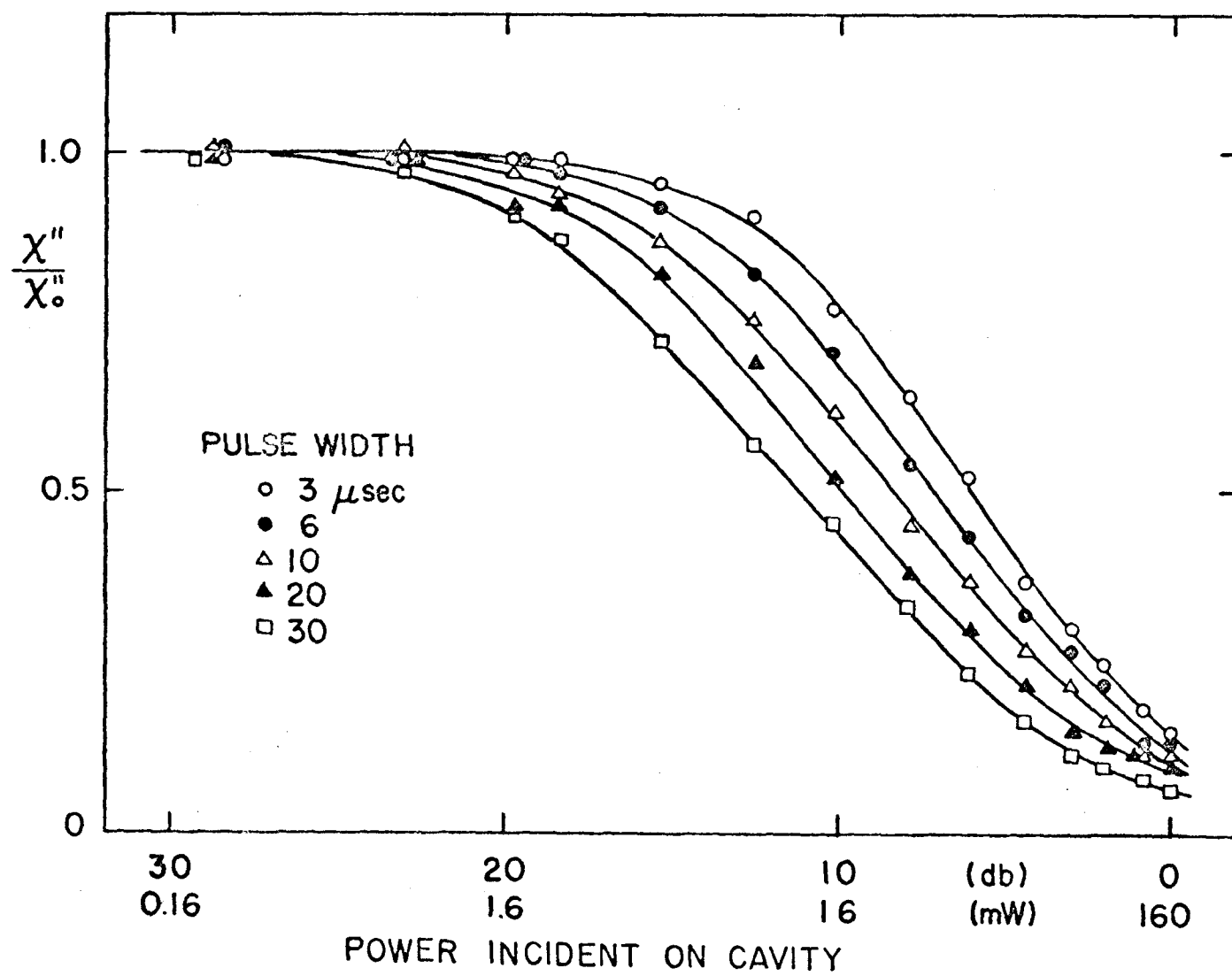


Fig. 29 Power dependence of χ'' at 1.4°K.

declines with both increasing microwave power level and increasing pulse width. The microwave magnetic field strength h_1 was determined from the cavity parameters and the microwave power using a formula

$$h_1^2 = \frac{Q_L P_c}{\omega_0 u} \frac{2}{1+\Gamma} \quad (22)$$

$$\text{and } u = \frac{V_c}{32\pi} \left(\frac{\lambda_g}{\lambda} \right)^2, \quad (23)$$

where Q_L is the loaded Q of the cavity, P_c is the power in the cavity, ω_0 is the microwave frequency, Γ is the cavity reflection coefficient (Γ^2 =power reflected/power incident), and V_c is the volume of the cavity. $Q_L=1400$, $P_c=150\text{mW}$, $\omega_0=8.9 \text{ kMc/sec}$, $u=1.24$, and $\Gamma=0.13$ were substituted in Eq.(22) and we obtain $h_1^2=0.34$, namely $h_1=0.6 \text{ Oe}$. Fig.29 shows h_c for the decline of χ'' to be about 0.06 Oe and this value and linewidth were substituted in Eq.(21). We obtain the spin-wave life time to be $6 \times 10^{-5} \text{ sec}$. This is in disagreement with T_{1a} of 10^{-7} sec order. Moreover, in Heeger's model of spin-wave instability, the induced magnetization M_z increases with increasing h_1 though χ'' declines at the same time. But our experimental result (Fig.24) shows that M_z at the end of the $10 \mu\text{sec}$ pulse declines with increasing h_1 near maximum input power. There is an ambiguity in the determination of χ'' and M_z because the resonance point shifts with both increasing h_1 and increasing pulse width. With varying H the maximum value of χ'' and M_z at MP_f was measured and so H did not satisfy the resonance condition at MP_1 because of the shift in the resonance position. Therefore the physical meaning of χ'' and M_z at MP_f is ambiguous and we cannot conclude whether the decline of χ'' in $\text{CuCl}_2 \cdot 2\text{H}_2\text{O}$ is due to the spin-wave instability or not.

The transverse component of the induced magnetization $M_{x,y}$ was observed and its relaxation time was determined as $T_2 \lesssim 5 \times 10^{-8} \text{ sec}$.

e) Energy transfer model.

Considering the facts described in the previous section, an energy transfer model inferred^r from the present experiment is as follows: The relaxation time of uniform precession ($k=0$) with spin-waves ($k \neq 0$) is very short and of the order of 10^{-8} sec because a very rapid transverse decay $T_2 \sim 10^{-8}$ sec was ascertained. This is also checked by ~~the fact that~~ the relaxation time calculated from the residual linewidth (6×10^{-8} sec). It should be noticed that the short relaxation does not accompany the longitudinal relaxation, namely, the decay of M_z . This means that the relaxation is the transition from $k=0$ magnon to $k \neq 0$ magnon with the conservation of M_z component. The possibility of direct decay to the lattice is not considered because the relaxation time T_{1a} is long enough compared to T_2 at low temperatures. Next the decay constant T_{1a} is considered. It may be clear that ^{the} M_z decay corresponds to the spin-lattice relaxation. In other words, T_{1a} means the relaxation time of $k \neq 0$ magnons. Finally the relaxation time T_{1b} corresponds with the decay time between lattice and bath, as was described in the previous section. A schematic block diagram of the energy transfer model is given by Fig.30.

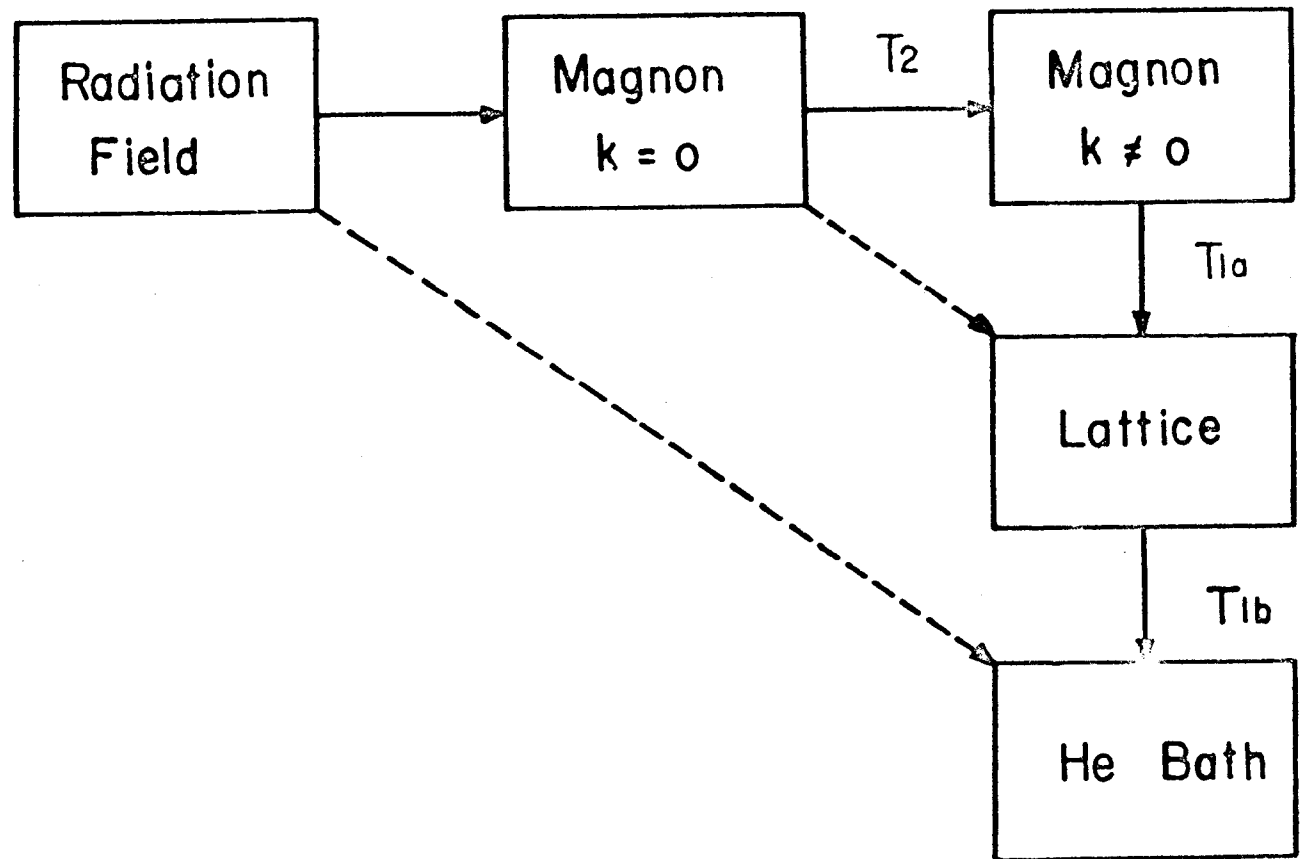


Fig.30 Schematic diagram of the transfer of energy.

5. New antiferromagnetic resonance lines in $\text{CuCl}_2\cdot 2\text{H}_2\text{O}$.

Detailed measurements of antiferromagnetic resonance in $\text{CuCl}_2\cdot 2\text{H}_2\text{O}$ were made by the Leiden group and their results were well understood by the theory developed by Nagamiya and Yosida and by Ubbink except for small deviations. Afterwards, Date and Nagata pointed out that ^{the} Δ main part of the deviations can be removed by introducing an inter-sublattice anisotropic exchange interaction in addition to the ordinary intra-sublattice anisotropy energy. The discrepancy still remained between the theory and experiment is the presence of a dip near the a-axis (spin easy axis) appearing in the resonance diagram of the ab-plane. (Fig.31.) During the study of the dip, we found new resonance lines in the ab-plane as shown by solid curves in Fig.31. They are weak and broad and are strongly angular dependent as shown in Figs.31 and 32. Moreover, they have asymmetric line shapes having steep tail on the lower field side. The experiments were performed at 1.4°K using microwaves of 9.0 and 4.2 kMc/sec with microwave powers less than 1 mW for both frequencies. It is noted that the new lines can be excited only by an rf-field perpendicular to the a-axis. The origin of the new resonance lines is not clear yet. It might be possible to explain the resonances by the following mechanism: near the dip, intra-sublattice spin canting angles due to the Dzyaloshinski-Moriya interaction are ^{of} Δ the order of 0.1~0.01 degree which may be smaller than that of an antiferromagnetic Larmor precession excited by a microwave. Accordingly, two equivalent canted states corresponding to two possible arrangements of canting spins in a ferromagnetic layer will be mixed, accompanying a new

k Oe

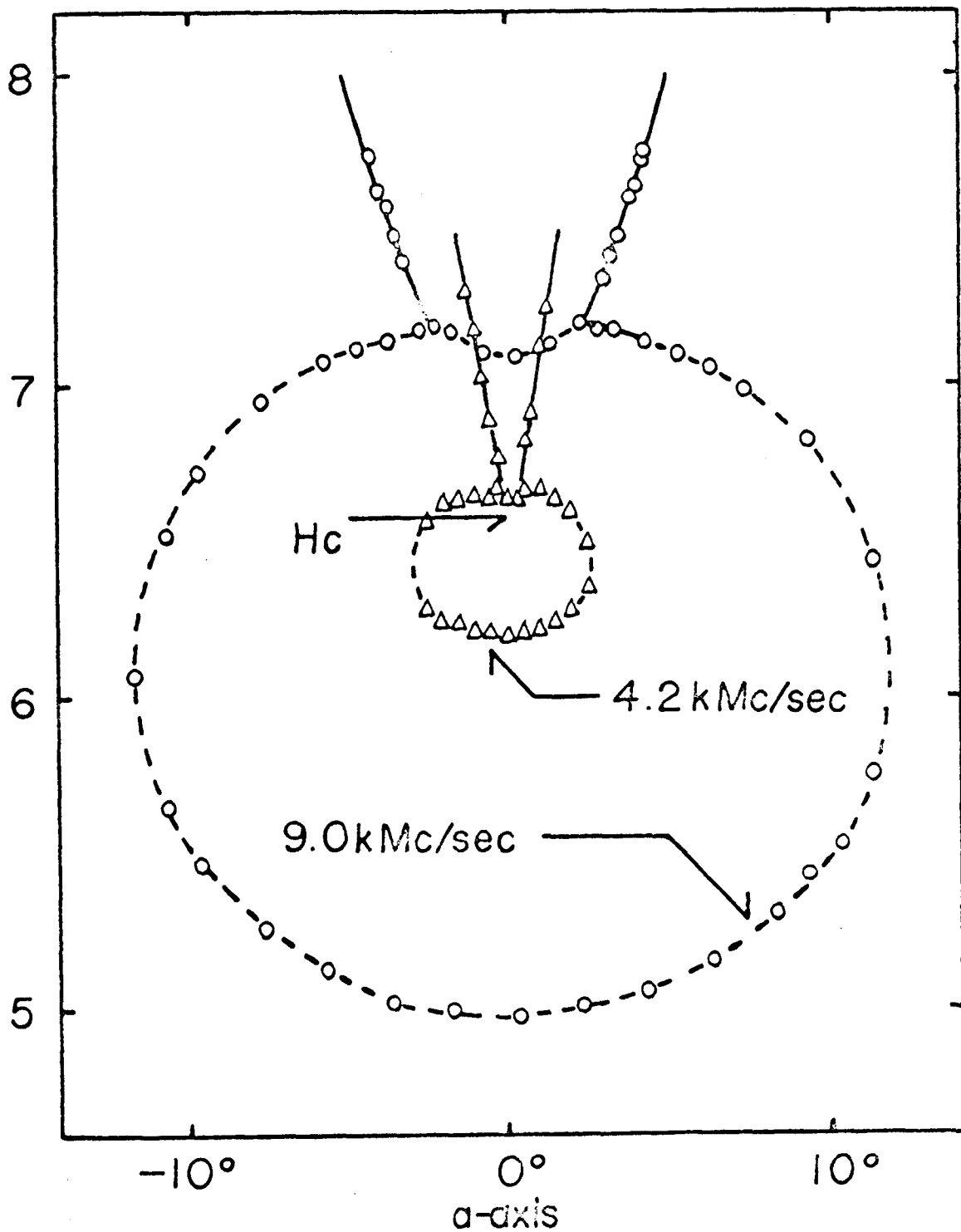


Fig.31 Resonance diagram in the ab -plane at 1.4°K . The solid curves show the new resonance lines and the dashed curves are the well known Nagamiya-Yosida lines.

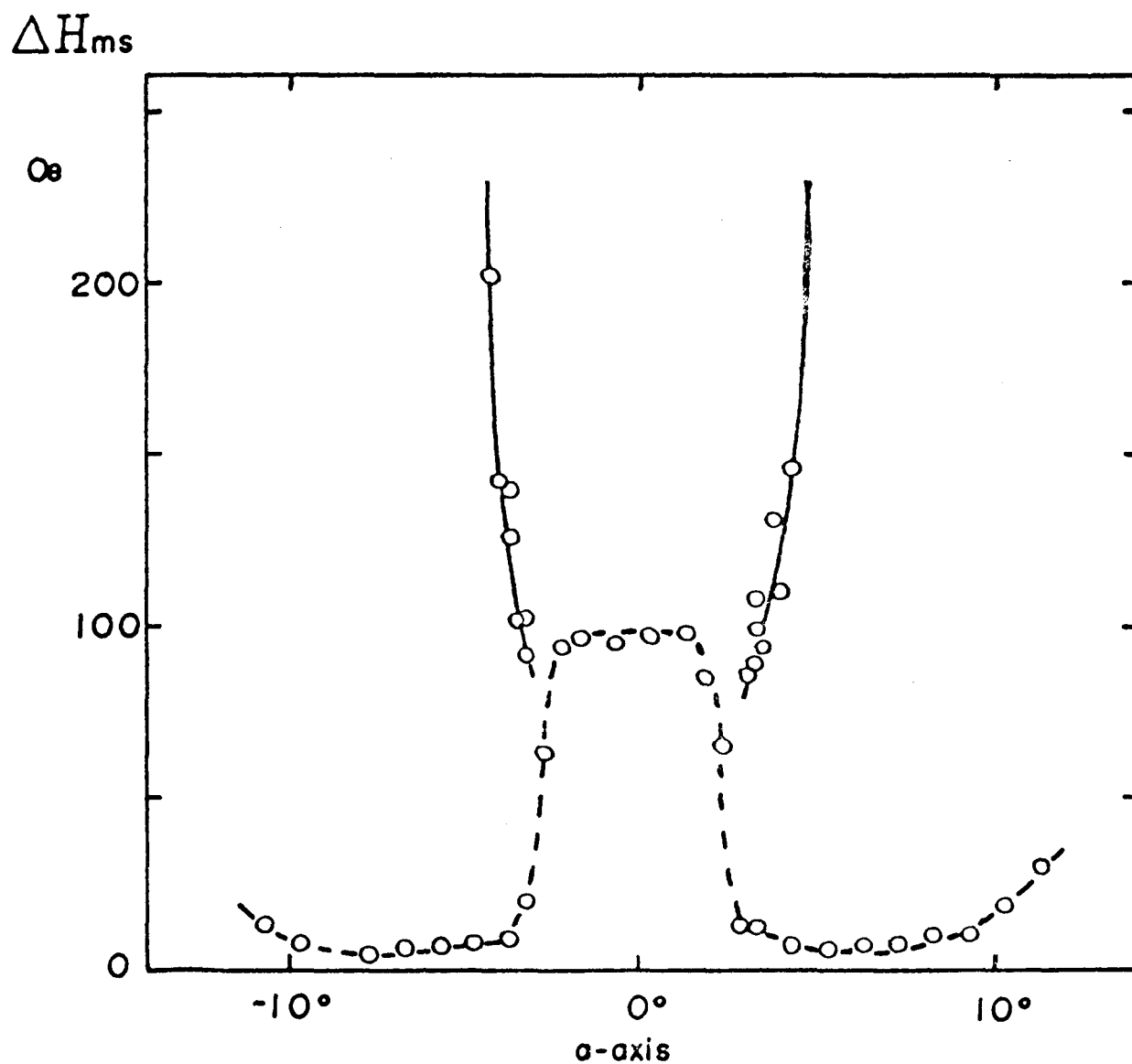


Fig.32 Observed full widths (maximum slope width) of the resonance lines at 9.0 kMc/sec(1.4°K). The solid curves show the new resonance linewidths and the dashed curves gives that of the Nagamiya-Yosida line near the dip.

resoance branch near the a-axis.

Now it may be said that there is a possibility to explain the origin of the dip in the ab-plane as a mixing effect of the well known Nagamiya-Yosida line and the new line. An anomalously broad line-width in the dip supports this possibility, since the resonance line in the branch well described by the Nagamiya-Yosida theory is very narrow giving a maximum-slope width of 6 Oe, as its narrowest case.

Acknowledgments.

The author wishes to express his sincere thanks to Prof. M.Date for his guidance throughout this work and to Prof. T.Nagamiya for reading the manuscript.

References.

- 1) H.J.Gerritsen, M.Garber, and G.W.J.Drews: *Physica* 22(1956) 213.
- 2) F.M.Johnson and A.H.Nethercot: *Phys. Rev.* 114(1959)705.
- 3) K.Nagata and M.Date: *J. Phys. Soc. Japan* 21(1966)2420.
- 4) V.N.Genkin and V.M.Fain: *Soviet Physics-JETP* 14(1962)1086.
- 5) T.Kawasaki: *Progr. theor. Phys.* 34(1965)357.
- 6) A.B.Harris: *J. appl. Phys.* 37(1966)1128.
- 7) K.Tani: *Progr. theor. Phys.* 31(1964)335.
- 8) K.Tomita and M.Tanaka: *Progr. theor. Phys.* 33(1965)1.
- 9) G.I.Urushadze: *Soviet Physics-JETP* 12(1961)476.
- 10) R.Loudon and P.Pincus: *Phys. Rev.* 132(1963)673.
- 11) U.N.Upadhyaya and K.P.Sinha: *Phys. Rev.* 130(1963)939.
- 12) H.Van Till and J.A.Cowan: *Bull. Amer. Phys. Soc.* 7(1962) 448.
- 13) A.J.Heeger: *Phys. Rev.* 131(1963)608.
- 14) A.S.Borovik-Romanov and L.A.Prozorova: *Soviet Physics-JETP* 19(1964)778.
- 15) V.I.Ozhogin: *Soviet Physics-JETP* 21(1965)874.
- 16) C.S.Naiman and T.R.Lawrence: *J. appl. Phys.* 36(1965)1161; *Phys. Letters* 14(1965)97.
- 17) R.W.Damon: *Rev. mod. Phys.* 25(1953)239.
- 18) N.Bloembergen and S.Wang: *Phys. Rev.* 93(1954)72.
- 19) L.C.Van der Marel, J. Van der Broek, J.D.Wasscher, and C. J.Gorter: *Physica* 21(1955)685.
- 20) S.A.Friedberg: *Physica* 18(1952)714.

- 21) N.J.Poulis and G.E.G.Hardeman: Physica 18(1952)201.
- 22) G.Shirane, B.C.Frazer, and S.A.Friedberg: Phys. Letters 17(1965)95.
- 23) H.Umebayashi, G.Shirane, B.C.Frazer, and D.E.Cox: to be published in J. appl. Phys.
- 24) The most complete accounts of the experimental results are contained in the thesis of J.Ubbink(1953) and that of H.J.Gerritsen(1955). These accounts are deplicated in a series of papers starting with that of N.J.Poulis, J.Van den Handel, J.Ubbink, and C.J.Gorter: Phys. Rev. 82(1952)552; the paper by J.H.Gerritsen and M.Garber: Physica 22(1956)418 gives later references.
- 25) M.Date and K.Nagata: J. appl. Phys. 34(1963)1038.
- 26) See for example, T.Nagamiya, K.Yosida, and R.Kubo: Advances in Phys. 4(1955)1.
- 27) J.Ubbink: Physica 19(1953)9.
- 28) H.Yamazaki and M.Date: J. Phys. Soc. Japan 21(1966)1615.
- 29) T.Moriya and K.Yosida: Progr. theor. Phys. 9(1953)663.
- 30) T.Moriya: Phys. Rev. 120(1960)91.
- 31) R.J.Joenk: Phys. Rev. 126(1962)565.
- 32) H.Yamazaki and M.Date: J. Phys. Soc. Japan 21(1966)1462.